Macromolecules

Article

pubs.acs.org/Macromolecules

Continuum Model for the Phase Behavior, Microstructure, and Rheology of Unentangled Polymer Nanocomposite Melts

Pavlos S. Stephanou,*[,†] Vlasis G. Mavrantzas,[‡,§] and Georgios C. Georgiou[†]

[†]Department of Mathematics and Statistics, University of Cyprus, PO Box 20537, 1678 Nicosia, Cyprus

[‡]Department of Chemical Engineering, University of Patras & FORTH-ICE/HT, Patras, GR 26504, Greece

[§]Department of Materials, Polymer Physics, ETH Zürich, HCI H 543, CH-8093 Zürich, Switzerland

Supporting Information

ABSTRACT: We introduce a continuum model for polymer melts filled with nanoparticles capable of describing in a unified and self-consistent way their microstructure, phase behavior, and rheology in both the linear and nonlinear regimes. It is based on the Hamiltonian formulation of transport phenomena for fluids with a complex microstructure with the final dynamic equations derived by means of a generalized (Poisson plus dissipative) bracket. The model describes the polymer nanocomposite melt at a mesoscopic level by using three fields (state variables): a vectorial (the momentum density) and two tensorial ones (the conformation tensor for polymer chains and the orientation tensor for nanoparticles). The dynamic equations are developed for nanoparticles with an arbitrary shape but then they are specified to the case of spherical ones. Restrictions on the parameters of the model are provided by analyzing its thermodynamic admissibility. A key ingredient of the model is the expression for the Helmholtz free energy A of the polymer nanocomposite. At equilibrium this reduces to the form introduced by Mackay et al. (*Science* **2006**, *311*, 1740−1743) to explain the phase behavior of polystyrene melts filled with silica nanoparticles. Beyond equilibrium, A contains additional terms that account for the coupling between microstructure and flow. In the absence of chain elasticity, the proposed evolution equations capture known models for the hydrodynamics of a Newtonian suspension of particles. A thorough comparison against several sets of experimental and simulation data demonstrates the unique capability of the model to accurately describe chain conformation and swelling in polymer melt nanocomposites and to reliably fit measured rheological data for their shear and complex viscosity over large ranges of volume fractions and deformation rates.

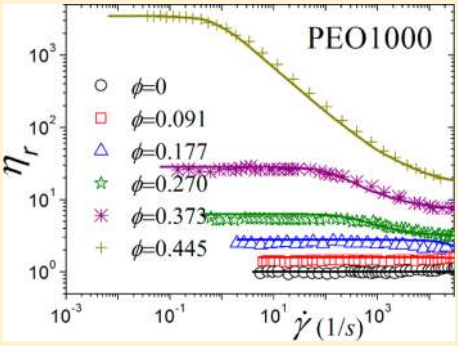

I. INTRODUCTION

Composite or heterogeneous materials can be found in abundance in nature. Two simple, nature-produced, polymer-based examples are wood (made up of fibrous chains of cellulose in a matrix of lignin) and bone (composed of hard inorganic crystals, hydroxyapatite, embedded in an organic matrix of collagen).[1] These materials find numerous applications in electronics, optics, catalysis, ceramics, and magnetic data storage devices.[2] Their widespread applications (from bulletproof vests to golf clubs, from vehicle tires to missile parts, etc.) has certainly integrated them into our lives.[3] Polymer matrix nanocomposites (PNCs), in particular, are hybrid organic/inorganic composites formed by the addition of nanoparticles to a polymer matrix, and blood and paint are only two of the numerous examples that demonstrate their importance.[4] Recent applications include use in solar photovoltaic devices,[5] in the development of lightweight materials for electrical applications,[6] and in diagnostics and therapy (e.g., as drug carriers to fight cancer[7]). At least one of the dimensions of the filler phase is in the nanometer scale leading to a large interfacial contact area with neighboring polymer chains. As a result, the composite material can have significantly improved properties relative to the pure polymer even at extremely small volume fractions (loadings) of the filler, and this has renewed interest in these systems in the past few years. Low-volume additions (1−10%) of isotropic (e.g., titania, alumina, and silver) or anisotropic (e.g., layered silicates, carbon nanotubes and nanofibers) nanoparticles result in significantly improved properties, comparable to those achieved via conventional loading (15−40%) of micrometer-scale inorganic fillers.[8] Materials with a variety of shapes may be employed as fillers in PNCs, such as nanoclays (primarily polymer-layered silicates, PLS),[9,10] nanoscopic silica particles,[9,11] nanotubes,[12] nanofibers,[13] and many others. This justifies the large number of simulation studies,[14,15] theories,[16] and rheological measurements[17] that have appeared recently in an effort to explain properties of this important class of materials and to understand fundamental issues related to chain dynamics in the vicinity of nanoparticle surface,[18,19] entanglement and disentanglement effects via primitive path analysis,[20,21] melt rheology,[22,23] and the importance of energetics and clustering.[24]

Received: February 25, 2014
Revised: May 23, 2014
Published: June 19, 2014

From the point of view of industrial applications, the interest lies in the rheological behavior of PNCs, with an emphasis on the dependence of the key material functions (shear viscosity, first and second normal stress coefficients, storage and loss moduli) on shear rate and nanoparticle volume fraction. The celebrated equation of Einstein[25] for the relative viscosity, namely $\eta_r = \eta/\eta_0 = 1 + (5/2)\phi$, where η denotes the viscosity of the suspension, η_0 the viscosity of the solvent, and ϕ the nanoparticle volume fraction, has been shown to accurately describe the rheological behavior of Newtonian spherical suspensions at low volume fractions ($\phi \sim 0.02$), provided interparticle interactions are neglected. Batchelor and Green[26] extended Einstein's equation to higher volume fractions ($\phi \sim 0.1$) by considering the effect of pairwise interactions and thus deriving the second-order term in the expansion of η_r with respect to ϕ; this correction has been verified experimentally.[27] Einstein's expression was extended to spheroids by Jeffery[28] who showed that the effective viscosity depends on particle orientation, namely $\eta_r = 1 + C\phi$, where C is a numerical parameter whose value depends on whether the spheroid is oblate or prolate. Hinch and Leal[29] computed an ensemble-averaged effective viscosity by including effects due to rotational diffusion. A general theory for dilute particle suspensions was put forth by Batchelor and Brenner.[30]

Most of the above hydrodynamic theories are limited to small volume fractions. Experimental data show that eventually the relative viscosity diverges at a volume fraction commonly denoted as the maximum packing fraction ϕ_T, which experimentally is found to lie in the range 0.55−0.71 [see, e.g., ref 31]. To account for this, simple empirical extensions have been proposed that employ a $1 - (\phi/\phi_T)$ term in the denominator. Such equations will be discussed later in this article.

For PNCs, the situation is more complicated: experimental observations fail to provide a satisfactory picture of their rheological behavior. Although early observations were in favor of an increased viscosity relative to the pure polymer,[32] evidence has been accumulated recently pointing (in many cases) to a reduced viscosity for PNCs when filled with spherical particles, which is unique only to this type of nanosized fillers. In particular, when fullerenes are added to monodisperse, linear, high molecular weight polysterene, the viscosity decreases,[33] an effect which has been attributed to the thermodynamic stability of the dispersion (this is attained only when the size of the fullerenes is smaller than the radius-of-gyration R_g of the polymer chains). The phenomenon seems to be connected with entanglement effects, since unentangled or nearly entangled systems (characterized by molecular weight $M_{mw} \sim M_c$, where M_c is the critical molecular weight at which entanglement effects become important) exhibit an increased zero shear rate viscosity when nanoparticles are added; in contrast, samples with M_{mw} exceeding M_c exhibit a reduced zero shear rate viscosity. Initially, this decrease was postulated to be related to the increase in the free volume of the melt caused by the addition of nanoparticles but later such an explanation was ruled out. According to Tuteja et al.,[33] the viscosity η_0 will decrease when (a) polymer chains are long enough to be entangled and (b) the average distance between nanoparticles is smaller than twice the polymer R_g. Additional experimental studies on poly(propylene) showed a similar decrease in the viscosity when silica nanoparticles were introduced into the matrix, which was attributed to the selective adsorption of high molecular weight polymer chains on the surface of silica.[34] Wang and Hill[35] explained this behavior by proposing (in the framework of a continuum hydrodynamic model) that in a PNC melt, a polymeric layer is formed in the neighborhood of the nanoparticle characterized by a smaller viscosity than the bulk polymer; the model, however, suffers from the assumption that the polymer matrix behaves as a Newtonian fluid. Needeless to say that, from a practical point of view, such a decrease in the viscosity would be highly desirable, since it implies that the processability of the material will be enhanced.

Starr et al.[36] have shown that the glass transition temperature T_g of a polymer melt can be shifted to either higher or lower temperatures by tuning the interactions between polymer and filler. The relaxation time of the radially averaged intermediate scattering function of the filled system should be larger than that of the unfilled one when the polymer−nanoparticle interactions are attractive (implying an increased T_g) but should decrease when the interactions are nonattractive (implying a decreased T_g).[36] The increase in relaxation time, which has also been observed in recent molecular dynamics (MD) simulations,[37] has been reported to be exponential.[15]

From the processing point of view, in addition to T_g, another important issue is that of miscibility, i.e., of the proper dispersion of nanoparticles in the polymeric matrix. Theoretical work by Hooper and Schweizer[38] has revealed two distinct spinodal curves: one at low nanoparticle−monomer attraction strengths associated with the formation of a thermodynamically stable polymer layer around nanoparticles (this is insensitive to nanoparticle size asymmetry ratio D/b_d with D and b_d denoting the nanoparticle diameter and monomer diameter or bead size, respectively) and a second one at higher attraction strengths associated with the formation of thermodynamically stable bridges as polymer segments connect different nanoparticles (this is more sensitive to the ratio D/b_d). The two spinodal curves are separated by a "miscibility window". These theoretical findings have also been confirmed by recent MD simulations.[39] The proper dispersion of spherical nanoparticles is typically associated with polymer swelling (the increase in the dimensions of polymer chains when nanoparticles are introduced in the polymer matrix).[34] This further motivated Mackay et al.[40] to propose a modified Flory−Huggins theory to describe the experimental findings.

Despite ample experimental[41] and simulation[15,18,21] evidence that the addition of nanoparticles induces polymer swelling, Crawford et al.[42] found that the ratio R_g/R_{g0} (where R_{g0} denotes the chain radius-of-gyration of the unfilled polymer) remains close to unity even up to $\phi \sim 0.35$. However, these authors have shown that for $R_g \leq a$ ($a = D/2$) PNCs phase separate whereas for $R_g > a$ a uniform dispersion should be obtained. Given that similar R_g/a ratios were used, the disagreement of their study with previous works [e.g., that of ref 40] suggests that polymer size may not be the only relevant parameter controlling chain swelling.

As far as the nonlinear rheology of PNCs is concerned, the works of Anderson and Zukoski[43,44] and Zhang and Archer[45] have shown that, following the linear viscoelastic (LVE) plateau, polymers filled with spherical nanoparticles exhibit a shear thinning behavior as the shear rate increases. Shear thinning occurs when hydrodynamic stresses prevail over thermodynamic ones,[43] resulting in a fast reduction of the viscosity with shear rate. By further increasing the shear rate, the viscosity curves for different volume fractions approach more and more that of the pure polymer. At very large shear rates, finally, the viscosity curves approach a plateau (an infinite

shear rate viscosity).[43] A similar shear-thinning behavior has been reported in the case of polymer melts filled with nanoclays[46] and nanofibers.[47]

In network theories,[48] physical entanglements between chains are considered as junctions between segments which may be destroyed and later recreated. Doremus and Piau[49] realized that the addition of nanoparticles would induce additional junctions due to adsorption of portions of chains on nanoparticles. Thus, a double network should emerge with different creation and destruction probabilities for each of the polymer−polymer and polymer−nanoparticle segments.[50] A similar double network approach has been adopted by Sarvestani and Picu[51] who derived expressions for the rates of chain attachment to and detachment from the nanoparticle; in a subsequent study, they used these expressions to introduce modifications to the friction coefficient of an encapsulated FENE dumbbell. Another kinetic theory approach was that of Xu et al.[52] where elastic dumbbells (being isotropic or anisotropic, with or without hydrodynamic interactions) were used to model nanofiber suspensions. It turns out that several authors[53] have proposed modifications to the reptation time due to chain attachment-detachment in the presence of nanoparticles.

In a number of more recent papers, Grmela and co-workers employed the GENERIC[54,55] formalism of nonequilibrium thermodynamics (NET) to describe the rheology of PNCs.[56−58] To model polymer chains they used the conformation tensor **C** while for the orientation of the fibers they employed a constrained (to reflect the constant length of fibers) orientation tensor **a** (both of these tensors will be discussed in due detail in the next section). Grmela and co-workers also made attempts to model nanoclay PNCs initially with the FENE-P model[56,57] and later by explicitly considering reptating chains.[46,58] To the best of our knowledge and despite several nonequilibrium thermodynamics studies of polymer−nanofiber and polymer−nanoclay systems, there has been no work addressing the case of polymer nanocomposite melts with nanospheres.

In this work, we introduce a rheological model for PNCs with spherical nanoparticles in the context of the generalized bracket formalism of NET,[59] by means of which several systems (primarily liquid crystals and polymers) and phenomena (such as polymer-wall interactions and polymer diffusion due to stress gradients in inhomogeneous flow fields) have been successfully addressed over the years.[55,59] Our approach (as well as that of Grmela and co-workers based on GENERIC) has the advantage that the final equations are developed in the context of a formalism which guarantees consistency with the first and second law of thermodynamics. In addition, it is very systematic (offering a unified description of phase behavior, transport phenomena and rheology) and can easily be coupled with a microscopic model for the underlying molecular interactions allowing for the full parametrization of the model. For practical applications, this is actually also the major disadvantage of the model, since it shows that it is not autonomous: for the complete description of the problem, additional input is required from lower-level simulations or models. We mention, for example, the expression for the free energy which should be independently derived from a microscopic model. Our aim in this study is ultimately to generalize our recent rheological model for homopolymers,[60,61] which has proven quite accurate in describing the results of direct atomistic non-equilibrium molecular dynamics (NEMD) simulations[60,61] and thermodynamically guided simulations at low and moderate shear rates,[62] to the more complex case of (unentangled or entangled) polymer matrices containing nanoparticles.

The paper is structured as follows: in section II a brief overview of the generalized bracket formalism of non-equilibrium thermodynamics is given. In section III, the new model is introduced: our choice of the state variables is discussed, the expression for the extended Helmholtz free energy is provided, and the full formulae for the Poisson and dissipation brackets are given. The dynamic equations for the case of spherical nanoparticles are derived and the model equations are reduced to known expressions in the limiting case of spherical particles dispersed in a Newtonian liquid. Also included in section III is the analysis of the thermodynamic admissibility of the model and the positive-definiteness of the conformation tensor. In section IV the expressions for the relevant rheological material functions obtained by analyzing the asymptotic behavior of the model in the limits of small shear and small uniaxial elongational flows are reported. In section V, the results obtained with the new model are presented: we first discuss its parametrization and then we show how accurately and reliably it can describe available experimental and simulation data for the shear viscosity of several PNC melts as a function of nanoparticle volume fraction over a wide range of shear rates. The paper concludes with section VI where the most important aspects of the new model are summarized and future plans are discussed.

At this point, we clarify that, in this work, (a) we have restricted ourselves to the case of well-dispersed nanoparticles in the polymer matrix and (b) we have used Einstein's implicit summation convention for any repeated Greek indices. We have also tried to keep in the paper only the most important material (equations and calculations) necessary to follow the presentation and derivation of the new model leaving technical (mostly mathematical) details for the accompanying Supporting Information.

II. NON-EQUILIBRIUM THERMODYNAMICS

In the context of classical mechanics, the appropriate set of state variables to consider for an N-particle system is $\mathbf{x} = \{\mathbf{r},\mathbf{p}\}$ with $\mathbf{r} = (\mathbf{r}_1,..,\mathbf{r}_N)$ and $\mathbf{p} = (\mathbf{p}_1,..,\mathbf{p}_N)$, where $\mathbf{r}_j$ and $\mathbf{p}_j$ denote the position and momentum vectors of the jth particle, respectively. Then, the time evolution of an arbitrary functional F is governed by Hamilton's equation of motion:[54,55,59,63]

$$\frac{\mathrm{d}F}{\mathrm{d}t} = \{F, E\} \tag{1}$$

where E is the total energy or the Hamiltonian H of the system and $\{.,.\}$ denotes the Poisson bracket. These systems are purely conservative, and the Poisson bracket has the bilinear form

$$\{F, E\} = \int \frac{\delta F}{\delta \mathbf{x}} \cdot \mathbf{L} \cdot \frac{\delta E}{\delta \mathbf{x}} \, \mathrm{d}^3\mathbf{r} \tag{2}$$

where $\mathbf{L}$ is the Poisson matrix.[54,55] The Poisson bracket must be antisymmetric $\{F,G\} = -\{G,F\}$, in order for the energy to be conserved, $\mathrm{d}E/\mathrm{d}t = 0$. It must also be time invariant and as such it should satisfy the Jacobi identity $\{F,\{G,P\}\} + \{G,\{P,F\}\} + \{P,\{F,G\}\} = 0$ for arbitrary functionals F, G and P.[54,55] In the literature, one can find guidelines and rules how to choose the Poisson bracket or, equivalently, the $\mathbf{L}$ matrix in order for the Jacobi identity to be automatically satisfied.[55] In addition, there is an automated code available online to check the Jacobi identity.[64]

dx.doi.org/10.1021/ma500415w | Macromolecules 2014, 47, 4493−4513

In actual applications, however, it is almost impossible to work with all degrees of freedom of the N-particle system. Instead, it is preferable to keep only a set of few slowly varying variables, meaning that fast degrees of freedom are averaged out, a procedure known as coarse-graining. Through such a procedure irrelevant degrees of freedom are eliminated at the expense of introducing entropy and dissipation.[65] To account then for the friction associated with the eliminated fast degrees of freedom, irreversibility must be added to the evolution equations at the coarse-grained level of description. Even when we start from a coarser (than the atomistic) level in which irreversible contributions have already been considered, additional irreversibility will be born when we will further coarse-grain by eliminating extra (fast) degrees of freedom. At this (coarse-grained) level of description, the evolution of state variables is elegantly separated as[55,63]

$$\frac{d\mathbf{x}}{dt} = \left.\frac{d\mathbf{x}}{dt}\right|_{reversible} + \left.\frac{d\mathbf{x}}{dt}\right|_{irreversible} \tag{3}$$

with the second contribution given (in a spirit similar to the first) as

$$\left.\frac{dF}{dt}\right|_{irreversible} = [F, S] \tag{4}$$

where S is the system's total entropy and $[.,.]$ denotes the dissipation bracket. Similar to eq 2, the latter is expressed as

$$[F, S] = \int \frac{\delta F}{\delta \mathbf{x}} \cdot \mathbf{M}_f \cdot \frac{\delta S}{\delta \mathbf{x}}\, d^3\mathbf{r} \tag{5}$$

where $\mathbf{M}_f$ is the friction matrix[54,55] associated with the increasing number of processes treated as fluctuations upon coarse-graining to slower and slower variables,[64] a direct consequence of the fluctuation−dissipation theorem. The dissipation bracket must be symmetric $[F,G] = [G,F]$ and positive semidefinite $[F,F] \geq 0$ in order for the evolution equation(s) to satisfy the second law of thermodynamics (the principle of non-negative rate-of-entropy production). Thus, we have a Poisson matrix $\mathbf{L}$ (or a Poisson bracket) that turns energy gradients into reversible dynamics and a friction matrix $\mathbf{M}_f$ (or a dissipation bracket) that turns entropy gradients into irreversible dynamics. To strictly separate reversible and irreversible contributions, the following mutual degeneracy requirements are further introduced:[54,55]

$$\{F, S\} = 0 \Rightarrow \mathbf{L} \cdot \frac{\delta S}{\delta \mathbf{x}} = 0$$
$$[F, E] = 0 \Rightarrow \mathbf{M}_f \cdot \frac{\delta E}{\delta \mathbf{x}} = 0 \tag{6}$$

The above conditions express the conservation of energy in the presence of dissipation and the conservation of entropy for any reversible dynamics.

Closely related to GENERIC is the generalized bracket approach,[59] a one-generator formalism expressed as

$$\frac{dF}{dt} = \{F, H\} + [F, H] \tag{7}$$

Except from subtle issues in the case of systems described (e.g.) by the Boltzmann equation[66] (i.e., through distribution functions) that favor GENERIC, the two formalisms are in complete agreement,[67] and thus may be used interchangeably.

A key issue in all nonequilibrium thermodynamics formalisms is the choice of state variables.[63,65] Althouth this is obvious when one deals with structureless media [in which case the state variables include the mass density ρ, the momentum density $\mathbf{M}$ (or the velocity $\mathbf{u} = \mathbf{M}/\rho$), and the energy density ε (or the entropy density s or the temperature T)], it is an issue of paramount importance when structured media are considered because of the additional internal variables that need to be considered in order to describe the microstructure of the system.[63] It is an issue requiring deep physical intuition and experience.[63] Typical choices for structural variables include a distribution function, the tensor of second moments of a distribution function, a scalar, etc.

III. GENERALIZED BRACKET BUILDING BLOCKS FOR POLYMER NANOCOMPOSITES

A. The Vector of State Variables. We restrict our analysis to the case of incompressible and isothermal polymer nanocomposites (the general case of compressible and nonisothermal systems is treated in the Supporting Information). Following the corresponding analysis for homopolymer melts,[60,61] the vector $\mathbf{x}$ of state variables is typically expressed as $\mathbf{x} = \{\mathbf{M}(\mathbf{r},t), \mathbf{C}(\mathbf{r},t), \mathbf{a}(\mathbf{r},t)\}$, where $\mathbf{M}$ is the momentum density, $\mathbf{C}$ the chain conformation tensor, and $\mathbf{a}$ the nanoparticle orientation tensor. $\mathbf{C}$ is defined as the tensor of the second moment of the distribution function $\Psi(\mathbf{R}_{ete},\mathbf{r},t)$ for the chain end-to-end vector $\mathbf{R}_{ete}$; i.e., $C_{\alpha\beta} \equiv \langle R_{ete,\alpha} R_{ete,\beta} \rangle = \int R_{ete,\alpha} R_{ete,\beta} \Psi(\mathbf{R}_{ete},\mathbf{r},t) d^3\mathbf{R}_{ete}$ with the brackets denoting a configurational average (see Figure 1). The spring constant is $K = 3k_BT/\langle R_{ete}^2 \rangle_{eq}^0$ where $\langle R_{ete}^2 \rangle_{eq}^0$ denotes the equilibrium mean-square end-to-end distance of the dumbbell in the pure homopolymer case. In the following, we will also employ the dimensionless conformation tensor $\tilde{\mathbf{C}}$ defined as $\tilde{C}_{\alpha\beta} \equiv 3C_{\alpha\beta}/\langle R_{ete}^2 \rangle_{eq}^0 = KC_{\alpha\beta}/k_BT$. We further clarify that at equilibrium, and contrary to Stephanou et al.,[60,61] $\tilde{\mathbf{C}}$ will not coincide with the unit tensor $\mathbf{I}$ but will be proportional to it; the proportionality constant will be evaluated below. The orientation tensor $\mathbf{a}$, on the other hand, is defined as $a_{\alpha\beta} \equiv \int n_\alpha n_\beta \psi(\mathbf{n},\mathbf{r},t) d^3\mathbf{n}$, where $\psi(\mathbf{n},\mathbf{r},t)$ denotes the orientational distribution function for the vector or director $\mathbf{n}$ at position $\mathbf{r}$ and time t (see Figure 1). The tensor $\mathbf{a}$ is constrained to have a constant trace, namely $\mathrm{tr}(\mathbf{a}) = A_0$ where A_0 is the surface area of the nanoparticle. For a sphere, $A_0 \approx D^2$, where D is its diameter while for nanofibers or nanotubes $A_0 \approx L^2$ where L is the length of the nanofiber or nanotube.[47] We also define the dimensionless orientation tensor $\tilde{\mathbf{a}} = (3/A_0)\mathbf{a}$ so that $\mathbf{a}_{eq} = (A_0/3)\mathbf{I}$, implying $\tilde{\mathbf{a}}_{eq} = \mathbf{I}$. At the coarse-grained level description of our model, the distribution functions $\Psi(\mathbf{R}_{ete},\mathbf{r},t)$ and $\psi(\mathbf{n},\mathbf{r},t)$ are only needed to define $\mathbf{C}$ and $\mathbf{a}$ (also to assign to them a clear physical interpretation); in the following only the tensors $\mathbf{C}$ and $\mathbf{a}$ will appear.

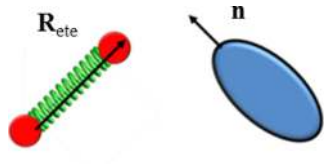

Figure 1. Polymer chains are modeled as dumbbells whose end-to-end distance vector $\mathbf{R}_{ete}$ defines the conformation tensor $\mathbf{C}$ and nanoparticles as spheroids for which the distribution of the director vector $\mathbf{n}$ defines their phase-space state through the orientation tensor $\mathbf{a}$.

B. The Hamiltonian. For incompressible and isothermal systems, the Hamiltonian is written as the sum of a kinetic energy K_{en} and a Helmholtz free energy term A:[59] $H_m = K_{en} + A = \int (\mathbf{M}^2/(2\rho)) d^3\mathbf{r} + A$. The latter is given here by the following expression:

$$A = A_{mix} + A_{pol} + A_{np} + A_{pol\text{-}np} \tag{8}$$

where A_{mix} denotes the free energy of nanoparticle−polymer mixing, A_{pol} is the elastic energy of polymer chains, A_{np} is the free energy due to nanoparticle orientation, and $A_{pol\text{-}np}$ is the free energy due to (enthalpic, steric, and topological) interactions between polymer chains and nanoparticles.

Free Energy of Mixing. For A_{mix}, we choose the modified Flory−Huggins expression proposed by Mackay et al.:[40]

$$\frac{v_{np}A_{mix}}{Vk_BT} = \chi\phi(1-\phi) + \phi \ln \phi + t_M(1-\phi)\ln(1-\phi) \tag{9}$$

where v_{np} denotes the volume of the nanoparticle, k_B the Boltzmann constant, χ the Flory mixing parameter, V the volume of the sample, ϕ the volume fraction of nanoparticles, and the parameter t_M is defined as $t_M = (D/2R_{g0})^3(\rho_p/\rho_0)$, where R_{g0} denotes the chain radius-of-gyration of the neat polymer at equilibrium, ρ_p the density of the neat polymer melt, and ρ_0 the density of a single polymer chain. Alternatively, the parameter t_M can be expressed as $t_M = v_{np}\rho_p N_{av}/M_{mw} = n_p^{pure}/n_a^{pure}$, where n_p^{pure} and n_a^{pure} denote the pure nanoparticle and pure polymer number densities, respectively. If ρ_p denotes the polymer mass density and N_{av} is the Avogadro number, then $n_p^{pure} = \rho_p N_{av}/M_{mw}$ and $n_a^{pure} = v_{np}^{-1}$. Equation 9 accounts for the Helmholtz free energy of mixing between polymer chains and nanoparticles and is able to describe (see Appendix A) the phase behavior of the nanocomposite in the sense that it can reproduce the bimodal obtained by Mackay et al.[40] An additional term called the Carnahan−Starling potential describing the nonideal part of the translational entropy of a hard-sphere gas can also been used,[68] but since it does not alter the phase behavior,[40] it will be omitted here. In general, the form of A_{mix} in our model has to be chosen with care, based on intuition and experience for the particular system at hand, because several different forms can be accommodated at our (coarse-grained) level of description.

Elastic Energy of Polymer Chains. For A_{pol} we have directly used the expression provided by Stephanou et al.[60,61] with a slight modification:

$$A_{pol} = \frac{n_p K[1+f(\phi)]}{2} \int \left\{ \Phi(\text{tr } \mathbf{C}) - \frac{k_BT}{K} \ln \det \tilde{\mathbf{C}} \right\} d^3\mathbf{r} \tag{10}$$

Equation 10 describes the total elastic energy of the polymer phase (as such, it is proportional to the polymer chain number density n_p) with polymer chains modeled as elastic (and, in general, nonlinear) springs with a spring constant K and a spring potential energy function Φ. This term is proportional to $f(\phi)$, a function which is introduced in order for the theory to be able to capture Einstein's equation for the viscosity of a Newtonian suspension of spherical particles. Indeed, with the form of eq 10 for A_{pol}, it turns out that the shear stress in shear flow is given by $\tau_{\alpha\beta} = \eta_0[1+f(\phi)]\dot{\gamma}_{\alpha\beta}$ (see section III.H). Therefore, by choosing $f(\phi) = (5/2)\phi$, we recover Einstein's formula for the reduced viscosity of a Newtonian suspension of hard spheres. Of course, one may employ any other functional form for f available from a lower-level theory or experiments.

Formally, there are two ways to reproduce Einstein's equation for the viscosity of a dilute suspension of nanoparticles using the generalized bracket: one is to add to the Hamiltonian a separate kinetic energy term for the particles due to their translational motion; the second is to consider (in addition to the linear momentum vector) the vorticity vector in the list of state variables and specify some additional coupling in the dissipation matrix (see examples 7.3 and 7.5 in ref 59). To keep the model simple, here we have used a third method: to use a multiplicative factor in the expression for the free energy due to polymer elasticity, implying an effective spring constant for polymer dumbbells in the presence of nanaparticles equal to the product of K with the function $f(\phi)$.

As far as the $-\ln \det \tilde{\mathbf{C}}$ term in eq 10 is concerned, this accounts for entropic contributions due to chain deformation by the flow. Note that for simplicity we have not made use of the $B(\mathbf{C})$ function employed by Stephanou et al.[60,61] For the spring potential we shall use the FENE-P(Cohen) expression, eq B5 in Appendix B, in which the finite extensibility parameter b is identified with $b = 3L_c^2/\langle R_{ete}^2\rangle_{eq}^0 = KL_c^2/k_BT$ (L_c being the contour length of the chain).

Free Energy Due to Nanoparticle Orientation. For the contribution to the free energy due to nanoparticle orientation, following Rajabian et al.[47] and Eslami et al.,[56] we use

$$A_{np} = \frac{n_a k_B T}{2} \int \left[\frac{3}{A_0}\text{tr}(\mathbf{a} - \mathbf{a}_{eq}) - \ln \det\left(\frac{3\mathbf{a}}{A_0}\right) - \frac{n_a\kappa}{9}\left(\frac{3}{A_0}\right)^2 [\text{tr}(\mathbf{a}^2) - (\text{tr } \mathbf{a})^2] \right] d^3\mathbf{r} \tag{11}$$

where n_a is the number density of nanoparticles and κ a parameter with dimensions of volume accounting for nanoparticle−nanoparticle interactions[56] whose magnitude is expected to be of the same order as the nanoparticle dimensions.

Polymer−Nanoparticle Interactions. The contribution to free energy due to polymer−nanoparticle interactions (enthalpic, steric, topological) is proportional to both n_p and n_a, and is expressed in terms of a single parameter κ' which (like κ) has dimensions of volume:[56]

$$A_{pol\text{-}np} = \frac{n_p k_B T}{2} \int \frac{n_a\kappa'}{A_0}\frac{K}{k_BT}[\text{tr}(\mathbf{C}\cdot\mathbf{a}) - (\text{tr } \mathbf{C})(\text{tr } \mathbf{a})]\, d\mathbf{r}^3 \tag{12}$$

As illustrated in section III.I, for the model to be thermodynamically admissible, the parameter κ' must be nonnegative ($\kappa' \geq 0$). Below, we will show that this parameter controls variations in the size of polymer chains due to nanoparticles: if $\kappa' = 0$, adding nanoparticles will have no effect on the size of chains (e.g., ref 42); if $\kappa' > 0$, adding nanoparticles to the polymer will cause chains to swell (e.g., ref 40).

Resulting Expression for the Free Energy. Putting all contributions to the free energy together, we obtain

dx.doi.org/10.1021/ma500415w | Macromolecules 2014, 47, 4493−4513

$$A = \frac{n_p K[1+f(\phi)]}{2}\int\left\{\Phi(\mathrm{tr}\,\mathbf{C}) - \frac{k_B T}{K}\ln\det\tilde{\mathbf{C}}\right\}\mathrm{d}^3\mathbf{r} + A_{\mathrm{mix}} + \frac{n_a k_B T}{2}\left(\frac{3}{A_0}\right)\int\left\{\frac{n_p\kappa'}{3}\frac{K}{k_B T}[\mathrm{tr}(\mathbf{C}\cdot\mathbf{a}) - (\mathrm{tr}\,\mathbf{a})(\mathrm{tr}\,\mathbf{C})]\right\}\mathrm{d}^3\mathbf{r} + \frac{n_a k_B T}{2}\left(\frac{3}{A_0}\right) \times \int\left\{\mathrm{tr}(\mathbf{a}-\mathbf{a}_{\mathrm{eq}}) - \frac{A_0}{3}\ln\det\left(\frac{3\mathbf{a}}{A_0}\right) - \frac{n_a\kappa}{9}\left(\frac{3}{A_0}\right) \times [\mathrm{tr}(\mathbf{a}^2) - (\mathrm{tr}\,\mathbf{a})^2] + \frac{2n_a\kappa}{3}\right\}\mathrm{d}^3\mathbf{r} \tag{13}$$

The last term in this equation (independent of the tensors $\mathbf{C}$ and $\mathbf{a}$) has been added so that at equilibrium this reduces exactly to the form proposed by Mackay et al.;[40] in the absence of flow, however, its contribution is irrelevant. It turns out that in the final transport equations the Volterra derivatives of A with respect to the tensors $\mathbf{C}$ and $\mathbf{a}$ are needed; expressions are provided in the Supporting Information. For high molecular weight polymers $b \gg 1$ implying that $h_{\mathrm{eq}} \approx 1$, and in this case—see eq SI.3a in the Supporting Information—one gets

$$\frac{\langle R_{\mathrm{ete}}{}^2\rangle_{\mathrm{eq}}}{\langle R_{\mathrm{ete}}{}^2\rangle^0_{\mathrm{eq}}} = \left(1 - \frac{2n_a\kappa'}{3[1+f(\phi)]}\right)^{-1} \tag{14a}$$

As will be shown in section III.I, strict thermodynamic arguments require that the parameter κ' must be non-negative. Then, eq 14a implies that the ratio $\langle R_{\mathrm{ete}}{}^2\rangle_{\mathrm{eq}}/\langle R_{\mathrm{ete}}{}^2\rangle^0_{\mathrm{eq}}$ of the equilibrium mean-square end-to-end distance of polymer chains in the presence and absence of nanoparticles is a nondecreasing function of ϕ: the dimensions of the chains will either remain the same (if $\kappa' = 0$) or increase (if $\kappa' > 0$), which supports the findings of Mackay et al.[40] How well eq 14a can reproduce the experimentally measured data of Mackay et al.[40] is discussed in Stephanou et al.[69] In the context of the present model, chain swelling is the net result of all possible interactions (steric, enthalpic, topological) between polymer chains and nanoparticles at our coarse-grained level of description, as embodied in the mesoscopic parameter κ'. For a very dilute suspension of nanoparticles in a melt of Gaussian chains ($b \gg 1$), eq 14a predicts the following linear relationship between degree of chain swelling and ϕ (irrespective of the particular form of the function $f(\phi)$):

$$\sqrt{\langle R_{\mathrm{ete}}{}^2\rangle_{\mathrm{eq}}/\langle R_{\mathrm{ete}}{}^2\rangle^0_{\mathrm{eq}}} \approx \sqrt{1+c_0\phi} \approx 1 + \frac{1}{2}c_0\phi \tag{14b}$$

where $c_0 = 2/3\kappa' n_a^{\mathrm{pure}}$.[69]

At this point, it is interesting to check the form of the expression for the free energy at equilibrium, for spherical nanoparticles. Setting $\mathbf{a} = \mathbf{a}_{\mathrm{eq}} = (3/A_0)\mathbf{I}$ in eq 13 and taking the equilibrium limit gives

$$A_{\mathrm{eq}} = \frac{n_p k_B T[1+f(\phi)]}{2}\int\left\{\mathrm{tr}\left(\frac{K}{k_B T}\mathbf{C}_{\mathrm{eq}} - \mathbf{I}\right) - \ln\det\tilde{\mathbf{C}}_{\mathrm{eq}}\right\}\mathrm{d}^3\mathbf{r} + A_{\mathrm{mix}} \tag{15a}$$

But $\mathrm{tr}((K/k_B T)\mathbf{C}_{\mathrm{eq}} - \mathbf{I}) = 3[(\langle R_{\mathrm{ete}}{}^2\rangle_{\mathrm{eq}}/\langle R_{\mathrm{ete}}{}^2\rangle^0_{\mathrm{eq}}) - 1]$, which leads to

$$A_{\mathrm{eq}} = \frac{3n_p k_B T[1+f(\phi)]}{2}\int\left\{\left(\frac{\langle R^2_{\mathrm{ete}}\rangle_{\mathrm{eq}}}{\langle R^2_{\mathrm{ete}}\rangle^0_{\mathrm{eq}}} - 1\right) - \ln\left(\frac{\langle R^2_{\mathrm{ete}}\rangle_{\mathrm{eq}}}{\langle R^2_{\mathrm{ete}}\rangle^0_{\mathrm{eq}}}\right)\right\}\mathrm{d}^3\mathbf{r} + A_{\mathrm{mix}}$$
$$\Rightarrow \frac{v_{\mathrm{np}}A_{\mathrm{eq}}}{Vk_B T} = \chi\phi(1-\phi) + \phi\ln\phi + t_M(1-\phi) \times \left\{\ln(1-\phi) + \frac{3[1+f(\phi)]}{2}c_0\phi\right\} \tag{15b}$$

the second line holding for small ϕ values for which eq 14b applies. Equation 15b demonstrates that at equilibrium we recover the free energy expression proposed by Mackay et al.[40] based on a modified Flory–Huggins theory for the description of the phase behavior of the polymer nanocomposite. For example, by considering the case of small ϕ and by setting the first derivative of A_{eq} with respect to ϕ equal to zero,[70] one obtains $\phi_B = \exp[-(1+\chi-(3c_0-1)t_M)]$, which is exactly the binodal proposed by Mackay et al.[40]

C. The Poisson Bracket. The expression for the Poisson bracket associated with the state variables $\mathbf{M}$ and $\mathbf{C}$ is well-known and can be found in many references.[55,59] For a conformation tensor $\mathbf{C}$, which is of the upper-convected type,[59] it reads

$$\{F,G\}^{MC} = -\int\left[\frac{\delta F}{\delta M_\gamma}\nabla_\beta\left(M_\gamma\frac{\delta G}{\delta M_\beta}\right) - \frac{\delta G}{\delta M_\gamma}\nabla_\beta\left(M_\gamma\frac{\delta F}{\delta M_\beta}\right)\right]\mathrm{d}^3\mathbf{r} - \int\left[\frac{\delta F}{\delta C_{\alpha\beta}}\nabla_\gamma\left(C_{\alpha\beta}\frac{\delta G}{\delta M_\gamma}\right) - \frac{\delta G}{\delta C_{\alpha\beta}}\nabla_\gamma\left(C_{\alpha\beta}\frac{\delta F}{\delta M_\gamma}\right)\right]\mathrm{d}^3\mathbf{r} + \int C_{\gamma\alpha}\left[\frac{\delta F}{\delta C_{\alpha\beta}}\nabla_\gamma\left(\frac{\delta G}{\delta M_\beta}\right) - \frac{\delta G}{\delta C_{\alpha\beta}}\nabla_\gamma\left(\frac{\delta F}{\delta M_\beta}\right)\right]\mathrm{d}^3\mathbf{r} + \int C_{\gamma\beta}\left[\frac{\delta F}{\delta C_{\alpha\beta}}\nabla_\gamma\left(\frac{\delta G}{\delta M_\alpha}\right) - \frac{\delta G}{\delta C_{\alpha\beta}}\nabla_\gamma\left(\frac{\delta F}{\delta M_\alpha}\right)\right]\mathrm{d}^3\mathbf{r} \tag{16a}$$

The additional part associated with the tensor $\mathbf{a}$ subject to the constraint $\mathrm{tr}(\mathbf{a}) = A_0$ can be derived (following Edwards et al.[71]) by starting with the corresponding Poisson bracket for the unconstrained orientation tensor $\hat{\mathbf{a}}$ (treated as an upper-convected type tensor):[47,56]

$$\{F,G\}^{\hat{a}} = -\int\left[\frac{\delta F}{\delta\hat{a}_{\alpha\beta}}\nabla_\gamma\left(\hat{a}_{\alpha\beta}\frac{\delta G}{\delta M_\gamma}\right) - \frac{\delta G}{\delta\hat{a}_{\alpha\beta}}\nabla_\gamma\left(\hat{a}_{\alpha\beta}\frac{\delta F}{\delta M_\gamma}\right)\right]\mathrm{d}^3\mathbf{r} + \int\hat{a}_{\gamma\alpha}\left[\frac{\delta F}{\delta\hat{a}_{\alpha\beta}}\nabla_\gamma\left(\frac{\delta G}{\delta M_\beta}\right) - \frac{\delta G}{\delta\hat{a}_{\alpha\beta}}\nabla_\gamma\left(\frac{\delta F}{\delta M_\beta}\right)\right]\mathrm{d}^3\mathbf{r} + \int\hat{a}_{\gamma\beta}\left[\frac{\delta F}{\delta\hat{a}_{\alpha\beta}}\nabla_\gamma\left(\frac{\delta G}{\delta M_\alpha}\right) - \frac{\delta G}{\delta\hat{a}_{\alpha\beta}}\nabla_\gamma\left(\frac{\delta F}{\delta M_\alpha}\right)\right]\mathrm{d}^3\mathbf{r} \tag{16b}$$

and by using the following *moment mapping* [see refs 59 and 71] to project the unconstrained tensor to a new one whose trace is constrained:

dx.doi.org/10.1021/ma500415w | Macromolecules 2014, 47, 4493–4513

$$\hat{\mathbf{a}} \rightarrow \mathbf{a} = A_0 \frac{\hat{\mathbf{a}}}{\mathrm{tr}\,\hat{\mathbf{a}}}$$

$$\frac{\delta}{\delta \hat{a}_{\alpha\beta}} = \frac{\partial a_{\gamma\epsilon}}{\partial \hat{a}_{\alpha\beta}} \frac{\delta}{\delta a_{\gamma\epsilon}} = \frac{A_0}{\mathrm{tr}\,\hat{\mathbf{a}}} \left(\delta_{\alpha\gamma}\delta_{\beta\epsilon} - \frac{a_{\gamma\epsilon}}{A_0}\delta_{\alpha\beta} \right) \frac{\delta}{\delta a_{\gamma\epsilon}} \tag{16c}$$

Through this, for the new tensor $\mathbf{a}$, the constraint $\mathrm{tr}(\mathbf{a}) = A_0$ holds automatically. By applying eqs 16c to 16b then we obtain

$$\begin{aligned}
\{F, G\}^a = &- \int \left[\frac{\delta F}{\delta a_{\alpha\beta}} \nabla_\gamma \left(a_{\alpha\beta} \frac{\delta G}{\delta M_\gamma} \right) - \frac{\delta G}{\delta a_{\alpha\beta}} \nabla_\gamma \left(a_{\alpha\beta} \frac{\delta F}{\delta M_\gamma} \right) \right] \mathrm{d}^3\mathbf{r} \\
&+ \int a_{\alpha\beta} \left[\frac{\delta F}{\delta a_{\alpha\beta}} \nabla_\gamma \left(\frac{\delta G}{\delta M_\gamma} \right) - \frac{\delta G}{\delta a_{\alpha\beta}} \nabla_\gamma \left(\frac{\delta F}{\delta M_\gamma} \right) \right] \mathrm{d}^3\mathbf{r} \\
&+ \int a_{\gamma\alpha} \left[\frac{\delta F}{\delta a_{\alpha\beta}} \nabla_\gamma \left(\frac{\delta G}{\delta M_\beta} \right) - \frac{\delta G}{\delta a_{\alpha\beta}} \nabla_\gamma \left(\frac{\delta F}{\delta M_\beta} \right) \right] \mathrm{d}^3\mathbf{r} \\
&+ \int a_{\gamma\beta} \left[\frac{\delta F}{\delta a_{\alpha\beta}} \nabla_\gamma \left(\frac{\delta G}{\delta M_\alpha} \right) - \frac{\delta G}{\delta a_{\alpha\beta}} \nabla_\gamma \left(\frac{\delta F}{\delta M_\alpha} \right) \right] \mathrm{d}^3\mathbf{r} \\
&- \frac{2}{A_0} \int a_{\alpha\beta} a_{\gamma\epsilon} \left[\frac{\delta F}{\delta a_{\gamma\epsilon}} \nabla_\alpha \left(\frac{\delta G}{\delta M_\beta} \right) - \frac{\delta G}{\delta a_{\gamma\epsilon}} \nabla_\alpha \left(\frac{\delta F}{\delta M_\beta} \right) \right] \mathrm{d}^3\mathbf{r}
\end{aligned} \tag{16d}$$

which is identical to the expression proposed by Eslami et al.[56] and Rajabian et al.[47]

Given the above expressions for the Poisson brackets, the following convective terms arise in the evolution equations of the state variables in our model (using that $\delta H_m/\delta \mathbf{M} = \mathbf{u}$):

$$\begin{aligned}
\left. \frac{\partial M_\alpha}{\partial t} \right|_{\text{convective}} &= -M_\gamma \nabla_\gamma u_\alpha - \nabla_\alpha p + \nabla_\gamma \tau_{\alpha\gamma}|_{\text{convective}} \\
\left. \frac{\partial C_{\alpha\beta}}{\partial t} \right|_{\text{convective}} &= -\nabla_\gamma (C_{\alpha\beta} u_\gamma) + C_{\gamma\alpha} \nabla_\gamma u_\beta + C_{\gamma\beta} \nabla_\gamma u_\alpha \\
\left. \frac{\partial a_{\alpha\beta}}{\partial t} \right|_{\text{convective}} &= -\nabla_\gamma (a_{\alpha\beta} u_\gamma) + a_{\gamma\alpha} \nabla_\gamma u_\beta + a_{\gamma\beta} \nabla_\gamma u_\alpha \\
&\quad - \frac{2}{A_0} a_{\alpha\beta} (a_{\gamma\epsilon} \nabla_\gamma u_\epsilon)
\end{aligned} \tag{16e}$$

where p denotes the thermodynamic pressure and

$$\tau_{\alpha\beta}|_{\text{convective}} = 2C_{\alpha\gamma} \frac{\delta A}{\delta C_{\gamma\beta}} + 2a_{\alpha\gamma} \frac{\delta A}{\delta a_{\gamma\beta}} - \frac{2}{A_0} a_{\alpha\beta} \left(a_{\gamma\epsilon} \frac{\delta A}{\delta a_{\gamma\epsilon}} \right) \tag{16f}$$

the convective part of the stress tensor $\boldsymbol{\tau}$.

D. The Dissipation Bracket. For the dissipation bracket, which is responsible for the additional terms in the final dynamic equations that specify the various transport processes and their couplings, the following most general expression (in terms of the tensors $\mathbf{C}$ and $\hat{\mathbf{a}}$) is used:

$$\begin{aligned}
[F, G]^{C\hat{a}} = &- \int \left[\frac{\delta F}{\delta C_{\alpha\beta}} \left(\Lambda^{CC}_{\alpha\beta\gamma\epsilon} \frac{\delta G}{\delta C_{\gamma\epsilon}} + \Lambda^{Ca}_{\alpha\beta\gamma\epsilon} \frac{\delta G}{\delta \hat{a}_{\gamma\epsilon}} \right) \right. \\
&\left. + \frac{\delta F}{\delta \hat{a}_{\alpha\beta}} \left(\Lambda^{Ca}_{\alpha\beta\gamma\epsilon} \frac{\delta G}{\delta C_{\gamma\epsilon}} + \Lambda^{aa}_{\alpha\beta\gamma\epsilon} \frac{\delta G}{\delta \hat{a}_{\gamma\epsilon}} \right) \right] \mathrm{d}^3\mathbf{r} \\
&+ \int L^C_{\alpha\beta\gamma\epsilon} \left[\frac{\delta F}{\delta C_{\gamma\epsilon}} \nabla_\alpha \left(\frac{\delta G}{\delta M_\beta} \right) - \frac{\delta G}{\delta C_{\gamma\epsilon}} \nabla_\alpha \left(\frac{\delta F}{\delta M_\beta} \right) \right] \mathrm{d}^3\mathbf{r} \\
&- \int Q_{\alpha\beta\gamma\epsilon} \nabla_\alpha \left(\frac{\delta F}{\delta M_\beta} \right) \nabla_\gamma \left(\frac{\delta G}{\delta M_\epsilon} \right) \mathrm{d}^3\mathbf{r} \\
&+ \int \tilde{L}^a_{\alpha\beta\gamma\epsilon} \left[\frac{\delta F}{\delta \hat{a}_{\gamma\epsilon}} \nabla_\alpha \left(\frac{\delta G}{\delta M_\beta} \right) - \frac{\delta G}{\delta \hat{a}_{\gamma\epsilon}} \nabla_\alpha \left(\frac{\delta F}{\delta M_\beta} \right) \right] \mathrm{d}^3\mathbf{r}
\end{aligned} \tag{17a}$$

The first term in the first integral involving $(\delta F/\delta C_{\alpha\beta})\Lambda^{CC}_{\alpha\beta\gamma\epsilon}(\delta G/\delta C_{\gamma\epsilon})$ and the entire second integral are the same with those proposed by Beris and Edwards[59] and used by Stephanou et al.[60,61] for pure homopolymer melts. To account for the constraint $\mathrm{tr}(\mathbf{a}) = A_0$, we can make again use of the *moment mapping* technique as we did for the Poisson bracket. Following Beris and Edwards,[59] we use

$$\frac{\delta}{\delta \hat{a}_{\alpha\beta}} = \left(\delta_{\alpha\gamma}\delta_{\beta\epsilon} - \frac{1}{3}\delta_{\gamma\epsilon}\delta_{\alpha\beta} \right) \frac{\delta}{\delta a_{\gamma\epsilon}} \tag{17b}$$

in the first integral and eq 16c in the last integral (together with $L^a_{\alpha\beta\gamma\epsilon} = \tilde{L}^a_{\alpha\beta\gamma\epsilon}(A_0/\mathrm{tr}\hat{\mathbf{a}})$) to find

$$\begin{aligned}
[F, G]^{Ca} = &- \int \left[\frac{\delta F}{\delta C_{\alpha\beta}} \left(\Lambda^{CC}_{\alpha\beta\gamma\epsilon} \frac{\delta G}{\delta C_{\gamma\epsilon}} + \Lambda^{Ca}_{\alpha\beta\gamma\epsilon} \frac{\delta G}{\delta a_{\gamma\epsilon}} - \frac{1}{3} \Lambda^{Ca}_{\alpha\beta\gamma\gamma} \frac{\delta G}{\delta a_{\zeta\zeta}} \right) \right. \\
&+ \frac{\delta F}{\delta a_{\alpha\beta}} \left(\Lambda^{Ca}_{\alpha\beta\gamma\epsilon} - \frac{1}{3} \Lambda^{Ca}_{\mu\mu\gamma\epsilon} \delta_{\alpha\beta} \right) \frac{\delta G}{\delta C_{\gamma\epsilon}} + \Lambda^{aa}_{\alpha\beta\gamma\epsilon} \left(\frac{\delta F}{\delta a_{\alpha\beta}} \frac{\delta G}{\delta a_{\gamma\epsilon}} \right. \\
&\left. \left. - \frac{1}{3} \frac{\delta F}{\delta a_{\zeta\zeta}} \delta_{\alpha\beta} \frac{\delta G}{\delta a_{\gamma\epsilon}} - \frac{1}{3} \frac{\delta G}{\delta a_{\zeta\zeta}} \delta_{\gamma\epsilon} \frac{\delta F}{\delta a_{\alpha\beta}} + \frac{1}{9} \frac{\delta F}{\delta a_{\zeta\zeta}} \frac{\delta G}{\delta a_{\theta\theta}} \delta_{\alpha\beta}\delta_{\gamma\epsilon} \right) \right] \mathrm{d}^3\mathbf{r} \\
&+ \int L^C_{\alpha\beta\gamma\epsilon} \left[\frac{\delta F}{\delta C_{\gamma\epsilon}} \nabla_\alpha \left(\frac{\delta G}{\delta M_\beta} \right) - \frac{\delta G}{\delta C_{\gamma\epsilon}} \nabla_\alpha \left(\frac{\delta F}{\delta M_\beta} \right) \right] \mathrm{d}^3\mathbf{r} \\
&- \int Q_{\alpha\beta\gamma\epsilon} \nabla_\alpha \left(\frac{\delta F}{\delta M_\beta} \right) \nabla_\gamma \left(\frac{\delta G}{\delta M_\epsilon} \right) \mathrm{d}^3\mathbf{r} \\
&+ \int L^a_{\alpha\beta\gamma\epsilon} \left[\frac{\delta F}{\delta a_{\gamma\epsilon}} \nabla_\alpha \left(\frac{\delta G}{\delta M_\beta} \right) - \frac{\delta G}{\delta a_{\gamma\epsilon}} \nabla_\alpha \left(\frac{\delta F}{\delta M_\beta} \right) \right] \mathrm{d}^3\mathbf{r} \\
&- \int L^a_{\alpha\beta\gamma\gamma} \frac{a_{\zeta\eta}}{A_0} \left[\frac{\delta F}{\delta a_{\zeta\eta}} \nabla_\alpha \left(\frac{\delta G}{\delta M_\beta} \right) - \frac{\delta G}{\delta a_{\zeta\eta}} \nabla_\alpha \left(\frac{\delta F}{\delta M_\beta} \right) \right] \mathrm{d}^3\mathbf{r}
\end{aligned} \tag{17c}$$

The first integral involves terms already presented by Grmela and co-workers,[47,56] whereas the rest are all new. The first accounts for relaxation effects in the nanocomposite through the fourth-rank semidefinite symmetric matrices $\boldsymbol{\Lambda}$: $\Lambda^{CC}_{\alpha\beta\gamma\epsilon}$ describes pure chain relaxation (inversely proportional to a characteristic chain relaxation time λ_p), $\Lambda^{aa}_{\alpha\beta\gamma\epsilon}$ describes pure nanoparticle relaxation (inversely proportional to a characteristic nanoparticle orientational relaxation time λ_a), and $\Lambda^{Ca}_{\alpha\beta\gamma\epsilon}$ describes coupled chain-nanoparticle relaxation (inversely proportional to a characteristic chain-nanoparticle relaxation time λ_{pa}, taken here as $\lambda_{pa} = (\lambda_p\lambda_a)^{1/2}$);[47,56] the terms

dx.doi.org/10.1021/ma500415w | Macromolecules 2014, 47, 4493−4513

proportional to 1/3 and 1/9, respectively, are direct consequences of the trace constraint. The terms involving the second, third and fourth integrals in eq 17c introduce a coupling between the velocity gradient and the conformation and orientation tensors through (again) fourth-rank tensors **L**: $L^{C}_{\alpha\beta\gamma\varepsilon}$ describes chain nonaffine motion[59] while $L^{a}_{\alpha\beta\gamma\varepsilon}$ is needed to provide the correct form of the evolution equation for nonspherical (but spheroidal) nanoparticles in the corresponding Jeffery equation.[28] As far as the term involving the fourth-rank tensor **Q** is concerned, this introduces an additional coupling between the velocity gradient and the orientation tensor which is important only for nonspherical nanoparticles and appears exclusively in the expression for the stress tensor.

E. The Evolution Equations. Calculating the contributions arising from the dissipative bracket and adding them up to those already calculated from the Poisson bracket, we arrive at the following full set of dynamic equations:

$$\frac{\partial \mathrm{M}_\alpha}{\partial t} = -M_\gamma \nabla_\gamma u_\alpha - \nabla_\alpha p - \nabla_\gamma \tau_{\alpha\gamma}$$

$$\frac{\partial C_{\alpha\beta}}{\partial t} = -u_\gamma \nabla_\gamma C_{\alpha\beta} + C_{\gamma\alpha}\nabla_\gamma u_\beta + C_{\gamma\beta}\nabla_\gamma u_\alpha + L^{C}_{\alpha\beta\gamma\varepsilon}\nabla_\gamma u_\varepsilon - \left[\Lambda^{CC}_{\alpha\beta\gamma\varepsilon}\frac{\delta A}{\delta C_{\gamma\varepsilon}} + \Lambda^{Ca}_{\alpha\beta\gamma\varepsilon}\left(\frac{\delta A}{\delta a_{\gamma\varepsilon}} - \frac{1}{3}\delta_{\gamma\varepsilon}\frac{\delta A}{\delta a_{\zeta\zeta}}\right)\right]$$

$$\frac{\partial a_{\alpha\beta}}{\partial t} = -u_\gamma \nabla_\gamma a_{\alpha\beta} + a_{\gamma\alpha}\nabla_\gamma u_\beta + a_{\gamma\beta}\nabla_\gamma u_\alpha - \frac{2}{A_0}a_{\alpha\beta}(a_{\gamma\varepsilon}\nabla_\gamma u_\varepsilon) + L^{a}_{\alpha\beta\gamma\varepsilon}\nabla_\gamma u_\varepsilon - \frac{a_{\alpha\beta}}{A_0}L^{a}_{\zeta\eta\gamma\gamma}\nabla_\zeta u_\eta - \left(\Lambda^{Ca}_{\alpha\beta\gamma\varepsilon} - \frac{1}{3}\Lambda^{Ca}_{\mu\mu\gamma\varepsilon}\delta_{\alpha\beta}\right)\frac{\delta A}{\delta C_{\gamma\varepsilon}} - \left[\left(\Lambda^{aa}_{\alpha\beta\gamma\varepsilon} - \frac{1}{3}\Lambda^{aa}_{\mu\mu\gamma\varepsilon}\delta_{\alpha\beta}\right)\frac{\delta A}{\delta a_{\gamma\varepsilon}} - \frac{1}{3}\left\{\Lambda^{aa}_{\alpha\beta\gamma\gamma} - \frac{1}{3}\Lambda^{aa}_{\zeta\zeta\theta\theta}\delta_{\alpha\beta}\right\}\frac{\delta A}{\delta a_{\mu\mu}}\right] \tag{18a}$$

We also obtain the following (complete now) equation for the stress tensor:

$$\tau_{\alpha\beta} = 2C_{\alpha\gamma}\frac{\delta A}{\delta C_{\gamma\beta}} + L^{C}_{\alpha\beta\gamma\varepsilon}\frac{\delta A}{\delta C_{\gamma\varepsilon}} + 2a_{\alpha\gamma}\frac{\delta A}{\delta a_{\gamma\beta}} - \frac{2}{A_0}a_{\alpha\beta}\left(a_{\gamma\varepsilon}\frac{\delta A}{\delta a_{\gamma\varepsilon}}\right) + L^{a}_{\alpha\beta\gamma\varepsilon}\frac{\delta A}{\delta a_{\gamma\varepsilon}} - \frac{a_{\zeta\eta}}{A_0}L^{a}_{\alpha\beta\gamma\gamma}\frac{\delta A}{\delta a_{\zeta\eta}} + Q_{\alpha\beta\gamma\varepsilon}\nabla_\gamma u_\varepsilon \tag{18b}$$

F. The Matrices L, Q, and Λ. To be able to use the above set of equations in actual calculations, we need to provide expressions for the fourth-rank tensors $\mathbf{\Lambda}^{CC}$, $\mathbf{\Lambda}^{aa}$, $\mathbf{\Lambda}^{Ca}$, $\mathbf{L}^{C}$, $\mathbf{L}^{a}$ and **Q**. For the **L** tensors, the following choices are made:

$$L^{C}_{\alpha\beta\gamma\varepsilon}(\mathbf{C}) = -\frac{\xi}{2}(C_{\alpha\gamma}\delta_{\beta\varepsilon} + C_{\alpha\varepsilon}\delta_{\beta\gamma} + C_{\beta\gamma}\delta_{\alpha\varepsilon} + C_{\beta\varepsilon}\delta_{\alpha\gamma}) \tag{19a}$$

$$L^{a}_{\alpha\beta\gamma\varepsilon}(\mathbf{a}) = \frac{\theta - 1}{2}(a_{\alpha\gamma}\delta_{\beta\varepsilon} + a_{\alpha\varepsilon}\delta_{\beta\gamma} + a_{\beta\gamma}\delta_{\alpha\varepsilon} + a_{\beta\varepsilon}\delta_{\alpha\gamma}) \tag{19b}$$

$L^{C}_{\alpha\beta\gamma\varepsilon}(\mathbf{C})$ describes nonaffine deformation effects for polymer chains through the so-called slip or nonaffine parameter ξ.[59−61] $L^{a}_{\alpha\beta\gamma\varepsilon}(\mathbf{a})$ introduces additional coupling between the orientation tensor and the velocity gradient field and in the form employed here it corresponds to Jeffery's equation with θ being a geometric parameter related to the nanoparticle aspect ratio through[28,72] $\theta = (\upsilon^2 - 1)/(\upsilon^2 + 1)$ where $\upsilon = l/D$ (l is the length and D the diameter of the cross-section of the nanoparticle); clearly, for spheres, $\theta = 0$.

The tensor **Q** is given by

$$Q_{\alpha\beta\gamma\varepsilon} = \frac{\eta_0(\phi)\phi}{A_0}\left[B(a_{\alpha\gamma}\delta_{\beta\varepsilon} + a_{\alpha\varepsilon}\delta_{\beta\gamma} + a_{\beta\gamma}\delta_{\alpha\varepsilon} + a_{\beta\varepsilon}\delta_{\alpha\gamma}) + \frac{2\bar{A}}{A_0}a_{\alpha\beta}a_{\gamma\varepsilon}\right] \tag{20}$$

and satisfies Onsager's relations: $Q_{\alpha\beta\gamma\varepsilon} = Q_{\beta\alpha\gamma\varepsilon} = Q_{\alpha\beta\varepsilon\gamma} = Q_{\gamma\varepsilon\alpha\beta}$. In eq 20, $\bar{A}$ and B are scalar functions of the geometric parameter θ which are available by Letwimolnun et al.[73] (in their notation $\bar{A} = A$).

For the relaxation matrices $\mathbf{\Lambda}^{CC}$, $\mathbf{\Lambda}^{aa}$ and $\mathbf{\Lambda}^{Ca}$ we have made the following choices:

$$\Lambda^{CC}_{\alpha\beta\gamma\varepsilon} = \frac{(1-\phi)}{2n_pK\lambda_p[1+f(\phi)]}(\tilde{\beta}_{\alpha\gamma}C_{\beta\varepsilon} + \tilde{\beta}_{\alpha\varepsilon}C_{\beta\gamma} + \tilde{\beta}_{\beta\gamma}C_{\alpha\varepsilon} + \tilde{\beta}_{\beta\varepsilon}C_{\alpha\gamma})$$

$$\Lambda^{aa}_{\alpha\beta\gamma\varepsilon} = \frac{A_0\Lambda^{aa}_0}{6\lambda_a n_a k_B T}(a_{\alpha\gamma}\delta_{\beta\varepsilon} + a_{\alpha\varepsilon}\delta_{\beta\gamma} + a_{\beta\gamma}\delta_{\alpha\varepsilon} + a_{\beta\varepsilon}\delta_{\alpha\gamma})$$

$$\Lambda^{Ca}_{\alpha\beta\gamma\varepsilon} = \frac{\Lambda^{Ca}_0(1-\phi)}{2\sqrt{\lambda_p\lambda_a}k_BT\sqrt{n_pn_a}}(a_{\alpha\gamma}C_{\beta\varepsilon} + a_{\alpha\varepsilon}C_{\beta\gamma} + a_{\beta\gamma}C_{\alpha\varepsilon} + a_{\beta\varepsilon}C_{\alpha\gamma}) \tag{21}$$

The relaxation tensor $\mathbf{\Lambda}^{CC}$ is very similar to that employed by Stephanou et al.[60,61] while for $\Lambda^{Ca}_{\alpha\beta\gamma\varepsilon}$ and $\Lambda^{aa}_{\alpha\beta\gamma\varepsilon}$ the simplest possible bilinear couplings have been chosen, namely $\Lambda^{Ca}_{\alpha\beta\gamma\varepsilon} \sim C_{\alpha\gamma}a_{\beta\varepsilon}$ and $\Lambda^{aa}_{\alpha\beta\gamma\varepsilon} \sim a_{\alpha\gamma}\delta_{\beta\varepsilon}$. Currently this is a postulate, but once NEMD simulation data are made available for these systems, we will be able to check their validity and properly modify them as we did in ref 60 for unfilled polymers. Also, $\mathbf{\Lambda}^{aa}_0$ and $\mathbf{\Lambda}^{Ca}_0$ in eq 21 denote numerical constants. Following Stephanou et al.,[60,61] the polymer chain longest relaxation time λ_p is allowed to depend on the conformation tensor via

$$\lambda_p = X(\phi)\lambda_0\lambda^*(\tilde{\mathbf{C}})$$
$$X(\phi) = \exp(x_{\mathrm{rel}}\phi)$$
$$\lambda^*(\tilde{\mathbf{C}}) = \exp(-\varepsilon\ \mathrm{tr}\ \tilde{\boldsymbol{\tau}}) \tag{22a}$$

Here λ_0 is the relaxation time of the pure polymer at equilibrium while the function $X(\phi)$ accounts for the dependence of chain relaxation time on nanoparticle volume fraction; and guided by recent simulation studies,[15,37] we have taken $X(\phi) = \exp(x_{\mathrm{rel}}\phi)$ where x_{rel} a numerical constant characteristic of the particular molecular system (polymer plus nanoparticles) under study. According to ref 15, $x_{\mathrm{rel}} = 8.98$ for volume fractions up to $\phi = 0.2$ (please note the typo in their eq 6 where instead of the common logarithm the natural one should have been used). A more recent simulation work[74] with unentangled polymer melts and roughly spherical nanoparticles suggests that (for nanoparticle volume fractions up to $\phi = 0.23$), $x_{\mathrm{rel}} = 1.1$. For the relaxation time of the nanoparticles, on the other hand, we have taken

dx.doi.org/10.1021/ma500415w | Macromolecules 2014, 47, 4493−4513

$$\lambda_a = Y(\phi)\lambda_0 \tag{22b}$$

with $Y(\phi) = \phi$ as suggested by Eslami et al.[56,58] It can be shown (see Appendix C) that this corresponds to the limiting case of a very dilute suspension of nanoparticles in the matrix. For the mobility tensor $\tilde{\boldsymbol{\beta}}$, a linear dependence on the stress tensor $\boldsymbol{\tau}$ is typically considered (see also Stephanou et al.[60,61]):

$$\tilde{\boldsymbol{\beta}} = \mathbf{I} + \alpha\tilde{\boldsymbol{\tau}} \tag{23}$$

with the magnitude of the Giesekus parameter α determining the degree of anisotropicity in the mobility of polymer chains due to their deformed shape by the flow field.

The expressions for Λ^{aa} and Λ^{Ca} are compatible with those of Eslami et al.[56] and Rajabian et al.[47] but not identical. For example, Eslami et al.[56] have adopted a similar expression for Λ^{aa} like ours (setting $f_1 = 1$ and $f_2 = f_3 = 0$ in their Λ^{aa}). They have also used a simpler expression for Λ^{CC}, since they have taken $\tilde{\boldsymbol{\beta}} = \mathbf{I} + \tilde{\mathbf{C}}$. Rajabian et al.,[47] on the other hand, have used similar expressions for Λ^{aa} and Λ^{Ca} but for Λ^{CC} they have taken $\tilde{\boldsymbol{\beta}} = \mathbf{I}$.

G. The Full Form of the Model. With the above choices, and using $\mathrm{tr}(\mathbf{a}) = A_0$, the evolution equations for C and $\mathbf{a}$ and the corresponding equation for the stress tensor $\boldsymbol{\tau}$ become

$$\begin{aligned}
\frac{\partial C_{\alpha\beta}}{\partial t} &= -u_\gamma\nabla_\gamma C_{\alpha\beta} + C_{\gamma\alpha}\nabla_\gamma u_\beta + C_{\gamma\beta}\nabla_\gamma u_\alpha \\
&- \frac{\xi}{2}(C_{\alpha\gamma}\dot{\gamma}_{\gamma\beta} + C_{\beta\gamma}\dot{\gamma}_{\gamma\alpha}) - \frac{(1-\phi)}{\lambda_p}\left\{\frac{1}{2}\left(h - \frac{n_a\kappa'}{1+f(\phi)}\right)\right. \\
&\times (\tilde{\beta}_{\alpha\gamma}C_{\beta\gamma} + \tilde{\beta}_{\beta\gamma}C_{\alpha\gamma}) - \frac{k_BT}{K}\tilde{\beta}_{\alpha\beta} + \frac{n_a\kappa'}{6[1+f(\phi)]}\left(\frac{3}{A_0}\right)a_{\varepsilon\gamma} \\
&\left.\times (\tilde{\beta}_{\alpha\gamma}C_{\beta\varepsilon} + \tilde{\beta}_{\beta\gamma}C_{\alpha\varepsilon})\right\} - \frac{\Lambda_0^{Ca}(1-\phi)}{\sqrt{\lambda_p\lambda_a}}\left(\frac{3}{A_0}\right)\sqrt{\frac{n_a}{n_p}}\left\{\frac{1}{2}\right. \\
&\times \left(1 + \frac{2n_a\kappa}{3} - \frac{n_p\kappa'}{3}\frac{K}{k_BT}\,\mathrm{tr}\,\mathbf{C}\right)(C_{\alpha\gamma}a_{\beta\gamma} + C_{\beta\gamma}a_{\alpha\gamma}) \\
&- \frac{A_0}{3}C_{\alpha\beta} - \frac{n_a\kappa}{9}\left(\frac{3}{A_0}\right)a_{\gamma\varepsilon}(C_{\alpha\gamma}a_{\beta\varepsilon} + C_{\beta\gamma}a_{\alpha\varepsilon}) \\
&+ \frac{n_p\kappa'}{3}\frac{K}{k_BT}\frac{1}{2}C_{\gamma\varepsilon}(C_{\alpha\gamma}a_{\beta\varepsilon} + C_{\beta\gamma}a_{\alpha\varepsilon}) \\
&- \frac{1}{6}(C_{\alpha\gamma}a_{\beta\gamma} + C_{\beta\gamma}a_{\alpha\gamma})\left[3 - \frac{A_0}{3}\,\mathrm{tr}\,\mathbf{a}^{-1} + \frac{4n_a\kappa}{3}\right. \\
&\left.\left. - \frac{2n_p\kappa'}{3}\frac{K}{k_BT}\,\mathrm{tr}\,\mathbf{C}\right]\right\}
\end{aligned} \tag{24a}$$

$$\begin{aligned}
\frac{\partial a_{\alpha\beta}}{\partial t} &= -u_\gamma\nabla_\gamma a_{\alpha\beta} + a_{\gamma\alpha}\nabla_\gamma u_\beta + a_{\gamma\beta}\nabla_\gamma u_\alpha \\
&+ \frac{\theta-1}{2}(a_{\alpha\gamma}\dot{\gamma}_{\gamma\beta} + a_{\beta\gamma}\dot{\gamma}_{\gamma\alpha}) - \frac{\theta}{A_0}a_{\alpha\beta}(a_{\gamma\varepsilon}\dot{\gamma}_{\gamma\varepsilon}) \\
&- \frac{\Lambda_0^{Ca}(1-\phi)K[1+f(\phi)]}{k_BT\sqrt{\lambda_p\lambda_a}}\sqrt{\frac{n_p}{n_a}} \\
&\times \left\{\frac{1}{2}\left(h - \frac{n_a\kappa'}{1+f(\phi)}\right)(a_{\alpha\gamma}C_{\beta\gamma} + a_{\beta\gamma}C_{\alpha\gamma}) - \frac{k_BT}{K}a_{\alpha\beta}\right. \\
&+ \frac{n_a\kappa'}{6[1+f(\phi)]}\left(\frac{3}{A_0}\right)a_{\varepsilon\gamma}(a_{\alpha\gamma}C_{\beta\varepsilon} + a_{\beta\gamma}C_{\alpha\varepsilon}) \\
&- \frac{\delta_{\alpha\beta}}{3}\left[\left(h - \frac{n_a\kappa'}{1+f(\phi)}\right)\mathrm{tr}(\mathbf{a}\cdot\mathbf{C}) - \frac{k_BT}{K}A_0\right. \\
&\left.\left.+\frac{n_a\kappa'}{3[1+f(\phi)]}\left(\frac{3}{A_0}\right)\mathrm{tr}(\mathbf{a}\cdot\mathbf{a}\cdot\mathbf{C})\right]\right\} \\
&- \frac{\Lambda_0^{aa}}{\lambda_a}\left\{\left[\left(1 + \frac{2n_a\kappa}{3} - \frac{n_p\kappa'}{3}\frac{K}{k_BT}\,\mathrm{tr}\,\mathbf{C}\right)a_{\alpha\beta} - \frac{A_0}{3}\delta_{\alpha\beta}\right.\right. \\
&- \frac{2n_a\kappa}{9}\left(\frac{3}{A_0}\right)a_{\alpha\gamma}a_{\beta\gamma} + \frac{n_p\kappa'}{6}\frac{K}{k_BT}(a_{\alpha\gamma}C_{\beta\gamma} + a_{\beta\gamma}C_{\alpha\gamma}) \\
&-\frac{\delta_{\alpha\beta}}{3}\left[\left(\frac{2n_a\kappa}{3} - \frac{n_p\kappa'}{3}\frac{K}{k_BT}\,\mathrm{tr}\,C\right)A_0 - \frac{2n_a\kappa}{9}\left(\frac{3}{A_0}\right)\mathrm{tr}(\mathbf{a}^2)\right. \\
&\left.\left.\left. + \frac{n_p\kappa'}{3}\frac{K}{k_BT}\,\mathrm{tr}(\mathbf{a}\cdot\mathbf{C})\right]\right\} + \frac{\Lambda_0^{aa}}{3\lambda_a}\left[3 - \frac{A_0}{3}\,\mathrm{tr}\,\mathbf{a}^{-1} + \frac{4n_a\kappa}{3}\right. \\
&\left.\left. - \frac{2n_p\kappa'}{3}\frac{K}{k_BT}\,\mathrm{tr}\,\mathbf{C}\right]\left(a_{\alpha\beta} - \frac{A_0}{3}\delta_{\alpha\beta}\right)
\end{aligned} \tag{24b}$$

and

$$\begin{aligned}
\tau_{\alpha\beta} &= (1-\xi)[1+f(\phi)]n_pK\left\{\left(h - \frac{n_a\kappa'}{1+f(\phi)}\right)C_{\alpha\beta}\right. \\
&\left. - \frac{k_BT}{K}\delta_{\alpha\beta} + \frac{n_a\kappa'}{6[1+f(\phi)]}\left(\frac{3}{A_0}\right)(a_{\alpha\gamma}C_{\beta\gamma} + a_{\beta\gamma}C_{\alpha\gamma})\right\} \\
&+ n_ak_BT\theta\left(\frac{3}{A_0}\right)\left\{\left[\left(1 + \frac{2n_a\kappa}{3} - \frac{n_p\kappa'}{3}\frac{K}{k_BT}\,\mathrm{tr}\,\mathbf{C}\right)a_{\alpha\beta}\right.\right. \\
&- \frac{A_0}{3}\delta_{\alpha\beta} - \frac{2n_a\kappa}{9}\left(\frac{3}{A_0}\right)a_{\alpha\gamma}a_{\gamma\beta} + \frac{n_p\kappa'}{6}\frac{K}{k_BT} \\
&\left.\left.\times (C_{\alpha\gamma}a_{\gamma\beta} + C_{\beta\gamma}a_{\gamma\alpha})\right] \right. \\
&- \frac{a_{\alpha\beta}}{A_0}\left[\left(\frac{2n_a\kappa}{3} - \frac{n_p\kappa'}{3}\frac{K}{k_BT}\,\mathrm{tr}\,\mathbf{C}\right)A_0 - \frac{2n_a\kappa}{9}\left(\frac{3}{A_0}\right)\mathrm{tr}\,\mathbf{a}^2\right. \\
&\left.\left. + \frac{n_p\kappa'}{3}\frac{K}{k_BT}\,\mathrm{tr}(\mathbf{a}\cdot\mathbf{C})\right]\right\} + \frac{\eta_0(\phi)\phi}{A_0}\left[\frac{\bar{A}}{A_0}\dot{\gamma}_{\gamma\varepsilon}a_{\alpha\beta}a_{\gamma\varepsilon}\right. \\
&\left. + B(\dot{\gamma}_{\alpha\gamma}a_{\gamma\beta} + a_{\gamma\alpha}\dot{\gamma}_{\gamma\beta})\right]
\end{aligned} \tag{24c}$$

dx.doi.org/10.1021/ma500415w | Macromolecules 2014, 47, 4493−4513

respectively. This set of equations is valid both under equilibrium and nonequilibrium conditions and provides a unified description of the coupling between microstructure and viscoelasticity in PNCs, irrespective of the value of nanoparticle volume fraction ϕ. It is thus capable of describing several sets of experimental data referring (e.g.) to particle dispersion, morphology, viscoelastic behavior, and response to a shear or extensional flow field. An alternative derivation of the model via the GENERIC formalism which avoids the assumptions of incompressible and isothermal fluid is presented in the Supporting Information.

H. Reduction to Simpler Cases. *Newtonian Suspension of Ellipsoidal Particles.* The case of ellipsoidal nanoparticles suspended in a Newtonian solvent is captured by choosing $\xi = 0$ (Newtonian fluids deform affinely), $\tilde{\mathbf{C}} = \mathbf{I}$ (thus also $\tilde{\beta}_{\alpha\beta} = \delta_{\alpha\beta}$), $\Lambda_0^{Ca} = 0$, $\kappa' = 0$ (thus also $\kappa = 0$), and $X(\phi) = 1$ (the relaxation time of a simple Newtonian fluid is negligible). Hence,

$$0 = \dot{\gamma}_{\alpha\beta} - \frac{(1-\phi)}{\lambda_0}(\tilde{C}_{\alpha\beta} - \delta_{\alpha\beta}) \Rightarrow \tilde{C}_{\alpha\beta} - \delta_{\alpha\beta} = \frac{\lambda_0 \dot{\gamma}_{\alpha\beta}}{(1-\phi)} \tag{25a}$$

$$\begin{aligned}\frac{\partial \bar{a}_{\alpha\beta}}{\partial t} &= -u_\gamma \nabla_\gamma \bar{a}_{\alpha\beta} + \bar{a}_{\gamma\alpha}\nabla_\gamma u_\beta + \bar{a}_{\gamma\beta}\nabla_\gamma u_\alpha \\ &+ \frac{\theta - 1}{2}(\bar{a}_{\alpha\gamma}\dot{\gamma}_{\gamma\beta} + \bar{a}_{\beta\gamma}\dot{\gamma}_{\gamma\alpha}) - \theta \bar{a}_{\alpha\beta}(\bar{a}_{\gamma\varepsilon}\dot{\gamma}_{\gamma\varepsilon}) \\ &- \frac{\Lambda_0^{aa}\,\mathrm{tr}(\bar{\mathbf{a}}^{-1})}{27\lambda_a}(3\bar{a}_{\alpha\beta} - \delta_{\alpha\beta})\end{aligned} \tag{25b}$$

where $\bar{\mathbf{a}} = \mathbf{a}/A_0 = \int \hat{\mathbf{n}}\hat{\mathbf{n}}\psi(\hat{\mathbf{n}}, \mathbf{r}, t)\mathrm{d}^3\hat{\mathbf{n}}$ (so that $\mathrm{tr}(\bar{\mathbf{a}}) = 1$). Choosing $\Lambda = \Lambda_0^{aa}\,\mathrm{tr}(\bar{\mathbf{a}}^{-1})/(27\lambda_a)$, eq 25b takes exactly the form that describes a Newtonian suspension [see, e.g., ref 73.]:

$$\begin{aligned}\frac{D\bar{a}_{\alpha\beta}}{Dt} &= \nabla_\gamma u_\alpha \bar{a}_{\gamma\beta} + \bar{a}_{\alpha\gamma}\nabla_\beta u_\gamma + \frac{1}{2}(\theta - 1)(\dot{\gamma}_{\alpha\gamma}\bar{a}_{\gamma\beta} + \bar{a}_{\gamma\alpha}\dot{\gamma}_{\gamma\beta}) \\ &- \theta\dot{\gamma}_{\varepsilon\gamma}\bar{a}_{\alpha\beta}\bar{a}_{\gamma\varepsilon} - \Lambda(3\bar{a}_{\alpha\beta} - \delta_{\alpha\beta})\end{aligned} \tag{25c}$$

The above choice for Λ is in accord with Folgar and Tucker,[72] who have suggested that $\Lambda = 2C_I\dot{\gamma}_0$ (i.e., that Λ should not be a constant). The corresponding expression for the stress tensor is

$$\begin{aligned}\tau_{\alpha\beta} &= n_p k_B T[1 + f(\phi)]\lambda_0(\tilde{C}_{\alpha\beta} - \delta_{\alpha\beta}) + 3\theta n_a k_B T \\ &\times \left(\bar{a}_{\alpha\beta} - \frac{1}{3}\delta_{\alpha\beta}\right) + \phi\eta_0[\bar{A}\dot{\gamma}_{\gamma\varepsilon}\bar{a}_{\alpha\beta}\bar{a}_{\gamma\varepsilon} \\ &+ B(\dot{\gamma}_{\alpha\gamma}\bar{a}_{\gamma\beta} + \bar{a}_{\gamma\alpha}\dot{\gamma}_{\gamma\beta})] \\ &= \eta_0\dot{\gamma}_{\alpha\beta} + 3\theta n_a k_B T\left(\bar{a}_{\alpha\beta} - \frac{1}{3}\delta_{\alpha\beta}\right) \\ &+ \eta_0\phi[\bar{A}\dot{\gamma}_{\gamma\varepsilon}\bar{a}_{\alpha\beta}\bar{a}_{\gamma\varepsilon} + B(\dot{\gamma}_{\alpha\gamma}\bar{a}_{\gamma\beta} + \bar{a}_{\gamma\alpha}\dot{\gamma}_{\gamma\beta}) + C\dot{\gamma}_{\alpha\beta}]\end{aligned} \tag{25d}$$

where we have used $f(\phi) = C\phi$ (see, e.g., Letwimolnun et al.[73]) in the final equation. The Newtonian viscosity is then identified with $\eta_0 = n_p^{\mathrm{pure}} k_B T \lambda_0$.

A Newtonian Suspension of Spherical Nanoparticles. Setting $\bar{\mathbf{a}} = \bar{\mathbf{a}}_{\mathrm{eq}} = (1/3)\mathbf{I}$ and $\theta = 0$ (meaning that $\bar{A} = B = 0$ and $C = 2.5$) in the above equation, we obtain

$$\tau_{\alpha\beta} = \eta_0\left(1 + \frac{5}{2}\phi\right)\dot{\gamma}_{\alpha\beta} \tag{26a}$$

i.e., we recover Einstein's equation for the viscosity of a Newtonian suspension of spherical particles. Actually, the model yields the following more general relation between stress and rate-of-strain tensors

$$\tau_{\alpha\beta} = \eta_0[1 + f(\phi)]\dot{\gamma}_{\alpha\beta} \tag{26b}$$

which agrees perfectly with several generalizations of Einstein's equation over the years:[31]

$$\begin{aligned} f(\phi) &= \frac{5}{2}\phi + 6.2\phi^2 \\ f(\phi) &= (1 + k\phi)^n - 1 \\ f(\phi) &= \left(1 - \frac{\phi}{\phi_T}\right)^{-2} - 1 \\ f(\phi) &= \left(1 - \frac{\phi}{\phi_T}\right)^{-(5/2)\phi} - 1 \end{aligned} \tag{26c}$$

The first corresponds to the second-order correction to Einstein's equation derived by Batchelor and Green[26] and the last with the empirical equation proposed by Krieger and Dougherty[75] for dense Newtonian suspensions.

A Polymer Melt Filled with Spherical Nanoparticles. For the more complex case of spherical nanoparticles dispersed in a polymeric fluid, we take $\bar{\mathbf{a}} = \bar{\mathbf{a}}_{\mathrm{eq}} = (1/3)\mathbf{I}$ and $\upsilon = 1$ (or, equivalently, $\theta = 0$, implying that $\bar{A} = B = 0$). The evolution equations then for the chain conformation tensor and nanoparticle orientation tensor assume the following form (in dimensionless units):

$$\begin{aligned}\frac{\partial \tilde{C}_{\alpha\beta}}{\partial t} &= -u_\gamma \nabla_\gamma \tilde{C}_{\alpha\beta} + \tilde{C}_{\gamma\alpha}\nabla_\gamma u_\beta + \tilde{C}_{\gamma\beta}\nabla_\gamma u_\alpha \\ &- \frac{\xi}{2}(\tilde{C}_{\alpha\gamma}\dot{\gamma}_{\gamma\beta} + \tilde{C}_{\beta\gamma}\dot{\gamma}_{\gamma\alpha}) - \frac{(1-\phi)}{\lambda_p} \\ &\times \left\{\frac{1}{2}\left(h - \frac{2n_a\kappa'}{3[1 + f(\phi)]}\right)(\tilde{\beta}_{\alpha\gamma}\tilde{C}_{\beta\gamma} + \tilde{\beta}_{\beta\gamma}\tilde{C}_{\alpha\gamma}) - \tilde{\beta}_{\alpha\beta}\right\} \\ &- \frac{\Lambda_0^{Ca}(1-\phi)}{\sqrt{\lambda_p\lambda_a}}\sqrt{\frac{n_a}{n_p}}\frac{n_p\kappa'}{3}\left(\tilde{C}_{\alpha\gamma}\tilde{C}_{\beta\gamma} - \frac{\mathrm{tr}\,\tilde{\mathbf{C}}}{3}\tilde{C}_{\alpha\beta}\right)\end{aligned} \tag{27a}$$

and

$$\begin{aligned}\frac{\Lambda_0^{aa}}{\lambda_a}\frac{n_p\kappa'}{3} &= -\frac{\Lambda_0^{Ca}(1-\phi)[1 + f(\phi)]}{\sqrt{\lambda_p\lambda_a}} \\ &\times \sqrt{\frac{n_p}{n_a}}\left(h - \frac{2n_a\kappa'}{3[1 + f(\phi)]}\right)\end{aligned} \tag{27b}$$

Equation 27b is needed in order to prove the thermodynamic admissibility of the model (see next section). As far as the stress tensor is concerned, this becomes

$$\begin{aligned}\tau_{\alpha\beta} &= (1 - \xi)n_p k_B T[1 + f(\phi)]\left\{\left[h - \frac{2n_a\kappa'}{3[1 + f(\phi)]}\right]\tilde{C}_{\alpha\beta}\right. \\ &\left. - \delta_{\alpha\beta}\right\}\end{aligned} \tag{27c}$$

dx.doi.org/10.1021/ma500415w | Macromolecules 2014, 47, 4493−4513

In the above equations, the nanoparticle and polymer number densities are given as $n_a = 6\phi/\pi D^3$ and $n_p = \rho_p(1-\phi)N_{av}/M_{mw}$, respectively. Equations 27a and 27c are the main results of this work.

I. Thermodynamic Admissibility and Positive Semi-definiteness of the Conformation Tensor. Any thermodynamic system has to satisfy the universal restriction of a non-negative total rate of entropy production. For incompressible and isothermal flows for which the entropy production results from the degradation of mechanical energy this restriction is expressed[59] as $dH_m/dt = [H_m, H_m] \leq 0$ (note the typo in Stephanou et al.,[60] section II.G). For this to be satisfied, we find that (see proof in the Supporting Information)

$$\begin{aligned} &n_p,\ \lambda_p \geq 0 \\ &0 \leq \xi < 1 \\ &0 \leq \alpha(1-\xi)[1+f(\phi)] \leq 1 \\ &\quad \Rightarrow 0 \leq \alpha \leq \{(1-\xi)[1+f(\phi)]\}^{-1} \\ &\Lambda_0^{Ca},\ n_a,\ \lambda_a \geq 0 \\ &0 \leq \kappa' \leq \frac{3}{2n_a}[1+f(\phi)] \end{aligned} \tag{28}$$

The constraints in eq 28 define the range of thermodynamically admissible values for the most important parameters of the proposed model. An alternative derivation of the thermodynamic admissibility of the new model is presented in the Supporting Information following the $C_M D C_M^T$ factorization scheme proposed by Edwards.[76]

The above set of constraints also guarantees the positive-definite nature of the tensor **C** (this is actually a prerequisite for checking thermodynamic admissibility). To see this, we follow Beris and Edwards[59] to bring first the evolution equation for **C** in the form

$$\begin{aligned} \frac{\partial \tilde{C}_{\alpha\beta}}{\partial t} &= -u_\gamma \nabla_\gamma \tilde{C}_{\alpha\beta} + \tilde{C}_{\gamma\alpha}\nabla_\gamma u_\beta + \tilde{C}_{\gamma\beta}\nabla_\gamma u_\alpha \\ &\quad - \frac{\xi}{2}(\tilde{C}_{\alpha\gamma}\dot{\gamma}_{\gamma\beta} + \tilde{C}_{\beta\gamma}\dot{\gamma}_{\gamma\alpha}) + \sum_{k=0}^{2} g_k(\tilde{C}^k)_{\alpha\beta} \end{aligned} \tag{29a}$$

by choosing

$$\begin{aligned} g_2(\tilde{C}) &= -\left(\frac{K}{k_B T}\right)^2 \left\{ \frac{\Lambda_0^{Ca}(1-\phi)}{\sqrt{\lambda_p \lambda_a}} \frac{n_p \kappa'}{3} \sqrt{\frac{n_a}{n_p}} \right. \\ &\quad \left. + \frac{(1-\phi)}{\lambda_p}\left(h - \frac{2n_a\kappa'}{3[1+f(\phi)]}\right)^2 \alpha(1-\xi)[1+f(\phi)] \right\} \\ g_1(\tilde{C}) &= \frac{K}{k_B T}\left\{ \frac{\Lambda_0^{Ca}(1-\phi)}{\sqrt{\lambda_p \lambda_a}} \frac{n_p \kappa'}{3} \sqrt{\frac{n_a}{n_p}} \frac{K}{k_B T} \frac{\mathrm{tr}\, C}{3} \right. \\ &\quad - \frac{(1-\phi)}{\lambda_p}\left(h - \frac{2n_a\kappa'}{3[1+f(\phi)]}\right)\{1 - 2\alpha(1-\xi) \\ &\quad \left. [1+f(\phi)]\}\right\} \\ g_0(\tilde{C}) &= \frac{(1-\phi)}{\lambda_p}\{1 - \alpha(1-\xi)[1+f(\phi)]\} \end{aligned} \tag{29b}$$

Then, a sufficient (but not necessary)[59] condition for C to be positive definite is $g_0(\tilde{C}) > 0$, which is true provided the constraints in eq 28 hold. We therefore conclude that the conditions for the thermodynamic admissibility of our model *and* the positive-definiteness of the tensor **C** are those dictated by eq 28.

IV. ASYMPTOTIC BEHAVIOR OF THE MODEL IN STEADY STATE SHEAR

In this section, we provide analytical expressions describing the asymptotic behavior of the new model in the limit of low deformation rates for the following two types of flow: steady shear flow (SSF) described by the kinematics $\mathbf{u} = (\dot{\gamma}_0 y, 0, 0)$ and uniaxial elongation flow (UEF) described by the kinematics $\mathbf{u} = (\dot{\varepsilon}_0 x, -0.5\dot{\varepsilon}_0 y, -0.5\dot{\varepsilon}_0 z)$, where x, y and z denote the three Cartesian coordinates. The material functions to be analyzed are the shear viscosity η $(= \tau_{xy}/\dot{\gamma}_0)$ and the two normal stress coefficients $\Psi_1 (= (\tau_{xx} - \tau_{yy})/\dot{\gamma}_0^2)$ and $\Psi_2 (= (\tau_{yy} - \tau_{zz})/\dot{\gamma}_0^2)$ in SSF, and the extensional viscosity $\eta_{1E} (= (\tau_{xx} - \tau_{yy})/\dot{\varepsilon}_0)$ in UEF. In SSF we find that

dx.doi.org/10.1021/ma500415w | Macromolecules 2014, 47, 4493−4513

$$\frac{\eta_0(\phi)}{\eta_0} \equiv \lim_{\lambda_0\dot{\gamma}_0\to 0}\frac{\eta}{\eta_0} = (1-\xi)^2(1-\phi)[1+f(\phi)] \times \frac{\tilde{H}_{eq}}{\tilde{H}_{eq}^2\tilde{\Lambda}_0^{CC}+\tilde{\Lambda}_0^{Ca}}$$

$$\frac{\Psi_{1,0}}{\eta_0\lambda_0} \equiv \lim_{\lambda_0\dot{\gamma}_0\to 0}\frac{\Psi_1}{\eta_0\lambda_0} = 2(1-\xi)^2(1-\phi)[1+f(\phi)] \times \left(\frac{\tilde{H}_{eq}}{\tilde{H}_{eq}^2\tilde{\Lambda}_0^{CC}+\tilde{\Lambda}_0^{Ca}}\right)^2$$

$$\frac{\Psi_{2,0}}{\eta_0\lambda_0} \equiv \lim_{\lambda_0\dot{\gamma}_0\to 0}\frac{\Psi_2}{\eta_0\lambda_0} = -(1-\xi)^2(1-\phi)[1+f(\phi)] \times \left(\frac{\tilde{H}_{eq}}{\tilde{H}_{eq}^2\tilde{\Lambda}_0^{CC}+\tilde{\Lambda}_0^{Ca}}\right)^3 \{\tilde{H}_{eq}\tilde{\Lambda}_0^{CC}[(1-\xi)\alpha_e+\xi] + \tilde{H}_{eq}^{-1}\tilde{\Lambda}_0^{Ca}\}$$

$$\frac{-\Psi_{2,0}}{\Psi_{1,0}} \equiv \lim_{\lambda_0\dot{\gamma}_0\to 0}\frac{-\Psi_2}{\Psi_1} = \frac{1}{2}(1-\phi)\frac{\tilde{H}_{eq}}{\tilde{H}_{eq}^2\tilde{\Lambda}_0^{CC}+\tilde{\Lambda}_0^{Ca}} \times \{\tilde{H}_{eq}\tilde{\Lambda}_0^{CC}[(1-\xi)\alpha_e+\xi] + \tilde{H}_{eq}^{-1}\tilde{\Lambda}_0^{Ca}\} \quad (30a)$$

In UEF we find that

$$\frac{\eta_{1E,0}(\phi)}{\eta_0} \equiv \lim_{\lambda_0\dot{\epsilon}_0\to 0}\frac{\eta_{1E}}{\eta_0} = 3(1-\xi)^2(1-\phi)[1+f(\phi)] \times \frac{\tilde{H}_{eq}}{\tilde{H}_{eq}^2\tilde{\Lambda}_0^{CC}+\tilde{\Lambda}_0^{Ca}} \quad (30b)$$

In the above expressions, $\eta_0 = n_p^{pure}k_BT\lambda_0$ denotes the viscosity of the Newtonian plateau while the quantities $\tilde{H}_{eq}$, $\tilde{\Lambda}_0^{CC}$and $\tilde{\Lambda}_0^{Ca}$ have been defined as $\tilde{H}_{eq} = h_{eq} - (2/3)n_a\kappa'[1+f(\phi)]^{-1}$, $\tilde{\Lambda}_0^{CC} = (1-\phi)/X(\phi)$, $\tilde{\Lambda}_0^{Ca} = (1-\phi)\Lambda_0^{Ca}(X(\phi)Y(\phi))^{-1}(1/3)\kappa'(n_pn_a)^{1/2}$. Equations 30 constitute generalizations of those introduced by Stephanou et al.[60] for pure homopolymers to the case of polymer nanocomposites. Equation 30b shows that the zero elongation rate extensional viscosity obeys Trouton's law, $\eta_{1E,0}(\phi) = 3\eta_0(\phi)$ for all ϕ.

We close section IV by noting that for melts of PNCs with spherical nanoparticles the model contains the following parameters:

1. the Giesekus parameter α accounting for anisotropic hydrodynamic drag in the constitutive equation for the conformation tensor
2. the PTT parameter ε controlling the variation of the longest chain relaxation time with chain conformation
3. the nonaffine parameter ξ accounting for the fact that individual chains will not deform affinely following macroscopically imposed flow field
4. the finite chain extensibility or FENE parameter b accounting for the finite size of real polymer chains
5. the chain longest relaxation time in the pure polymer melt, λ_0
6. the parameter κ' describing polymer−nanoparticle interactions
7. the parameter x_{rel} describing the dependence of polymer relaxation time on nanoparticle volume fraction
8. the parameter Λ_0^{Ca} entering the expression for the relaxation matrix; this controls the coupling between the two structural variables

Parameters 1−5 are needed to capture correctly the rheological response of the neat polymer matrix (both in shear and elongation), and should be known prior to analyzing the PNC case. Then, one is left with three unknown parameters only, the set $\{x_{rel}, \kappa', \Lambda_0^{Ca}\}$, whose values must be specified either through comparison with experimental data or by carrying out independent molecular simulations for the specific polymer nanocomposite melt.

It turns out that the above set can be reduced even more, since one can obtain a good estimate for κ' (accounting, effectively, for nanoparticle-mediated excluded volume interactions) in terms of just the diameter D of the nanoparticles and the equilibrium radius-of-gyration R_{g0} of the polymer chains. The analysis is carried out in the Supporting Information and the main idea is to treat the term proportional to tr(**C**·**a**) − (tr **a**)(tr **C**) in eq 12 as a Maier−Saupe type of entropy by generalizing the approach presented by Khokhlov and Semenov[77] to the case of a hard spheroidal nanoparticle and a soft polymer coil. We find (see the Supporting Information)

$$\kappa' \cong \sqrt{6}(b_d + D)DR_{g0} \quad (31)$$

which is an extremely useful expression, since it provides a very good estimate for κ' in terms of geometric factors for nanoparticles and polymer chains.

Alternatively, one can precisely fix the value of κ' but also of the other two parameters (x_{rel} and Λ_0^{Ca}) from independent NEMD simulations. To see how this can be done, we can analyze the asymptotic behavior of the model predictions for the elements of the conformation tensor in the limit of small shear rates to come up with the following set of equations in the case of simple shear flow:

$$\tilde{C}_{xx} = \tilde{H}_{eq}^{-1} - \frac{k^2\tilde{H}_{eq}}{1-\xi}\{(\tilde{H}_{eq}{}^2\alpha_e\tilde{\Lambda}_0^{CC} + \tilde{\Lambda}_0^{Ca})k + \xi - 2\}We^2 \quad (32a)$$

$$\tilde{C}_{xy} = kWe \quad (32b)$$

$$\tilde{C}_{yy} = \tilde{H}_{eq}{}^{-1} - \frac{k^2\tilde{H}_{eq}}{1-\xi}\{(\tilde{H}_{eq}{}^2\alpha_e\tilde{\Lambda}_0^{CC} + \tilde{\Lambda}_0^{Ca})k + \xi - 2\}We^2 \quad (32c)$$

and

$$\tilde{C}_{zz} = \tilde{H}_{eq}{}^{-1} \quad (32d)$$

where $k = (1-\xi)[\tilde{H}_{eq}{}^2\tilde{\Lambda}_0^{CC} + \tilde{\Lambda}_0^{Ca}]^{-1}$, $\alpha_e = \alpha(1-\xi)[1+f(\phi)]$, and $We = \lambda_0\dot{\gamma}_0$ denotes the dimensionless shear rate. Similar expressions can be obtained for UEF. These expressions are consistent with what is known about the dependence of viscometric functions on shear rate in simple shear flows: the nondiagonal component C_{xy} increases linearly with We while the two diagonal ones C_{xx} and C_{yy} increase quadratically with We.[78] But what is more interesting is that these constitute a system of four algebraic equations in four unknowns (κ', Λ_0^{Ca}, x_{rel}, $f(\phi)$); therefore, one can utilize independent NEMD simulation data for a given polymer−nanoparticle melt to obtain κ', Λ_0^{Ca}, x_{rel}, and $f(\phi)$, thus totally avoiding the need for any fitting.

dx.doi.org/10.1021/ma500415w | Macromolecules 2014, 47, 4493−4513

V. RESULTS

All predictions of the new model discussed in this Section have been obtained with the FENE-P(Cohen) approximation for the function h needed in eqs 27a and 27c, since this provides a better description of available rheological data for the corresponding neat homopolymers than the Warner approximation.[60,61] We have also used the following parameter values referring to the polymer component: $\alpha = 0.05$, $\xi = \varepsilon = 0.01$, $b = 50$ and $\rho_p = 1\text{gr/cm}^3$. We have further employed Einstein's formula for the function f, namely $f(\phi) = (5/2)\phi$. Our goal then is to discuss how the addition of nanoparticles alters the viscometric functions of the melt in SSF and UEF, and how it affects the components of the conformation tensor. Recall that for the neat polymer melt, the zero shear rate viscosity is given by $\eta_p = \eta_0(1 - \xi)^2$.[60,61] The results will be analyzed in terms of nanoparticle volume fraction ϕ, for several values of the set of parameters $\{x_{rel}, \kappa', \Lambda_0^{Ca}\}$. Most of the results have been obtained for nanoparticles with diameter $D = 1$ nm and molecular weight $M_{mw} = 1000$ g/mol, but some additional results for different values of M_{mw} and D will also be presented.

A. Material Functions in Simple Shear. Figure 2 shows the variation of the relative zero shear rate viscosity $\eta_r = \eta/\eta_p$

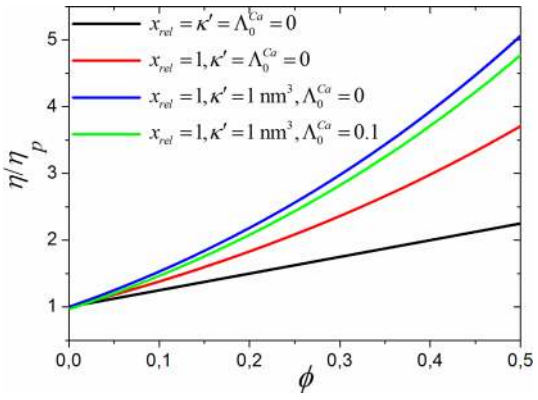

Figure 2. Model predictions for the relative zero shear rate viscosity η_r of a PNC for different values of the set of model parameters $\{x_{rel}, \kappa', \Lambda_0^{Ca}\}$. In the particular case that all these parameters are zero, the model reproduces Einstein's formula for the viscosity (i.e., $\eta_r = 1 + {}^5/_2\phi$).

with ϕ for different values of the set $\{x_{rel}, \kappa', \Lambda_0^{Ca}\}$. When both κ' and Λ_0^{Ca} are zero, η_r follows the Einstein formula as expressed by eq 30a. By introducing $x_{rel} = 1$ (i.e., by allowing for an exponential increase in the polymer longest relaxation time with nanoparticle volume fraction), eq 30a shows that η_r increases also exponentially with ϕ. Assuming a nonzero value for κ' (e.g., using $\kappa' = 1\ \text{nm}^3$) is then sufficient to further push the curves upward (since $\tilde{H}_{eq} < 1$). For example, for $\phi = 0.5$ and $\kappa' = 0$ the relative zero shear rate shear viscosity η_r is ~3.7 whereas for $\phi = 0.5$ and $\kappa' = 1\ \text{nm}^3$ the value of η_r increases to ~5.1. The effect of Λ_0^{Ca}, on the other hand, is to shift the curve downward.

In Figure 3 we present the growth of the shear viscosity upon inception of shear flow for three different values of We: $We = 0.1$, 1, and 10. In Figure 3a, the results are compared for two different volume fractions: $\phi = 0$ (corresponding to the pure polymer melt) and $\phi = 0.1$ (corresponding to a PNC with a low concentration in nanoparticles). The numerical data have been obtained for $\Lambda_0^{Ca} = \kappa' = x_{rel} = 0$. For small We values, the results can be easily obtained by solving the model in the linear viscoelastic (LVE) regime, i.e., by using $\eta_0(\phi)[1 - \exp(-t/\lambda(\phi))]$ where $\lambda(\phi) = \lambda_0\tilde{H}_{eq}[\tilde{H}_{eq}^2\tilde{\Lambda}_0^{CC} + \tilde{\Lambda}_0^{Ca}]^{-1}$ and $\eta_0(\phi)$ is given by the first formula in eq 30a. For the pure polymer melt, $\eta_0(\phi = 0) = \eta_p$. The figure shows that for $We = 0.1$ the viscosity initially increases equally in the two systems, but the resulting steady-state values are different (since they depend on ϕ). Despite the fact that these steady-state viscosity values are strong functions of ϕ, as the We increases, the model predicts similar values between the pure polymer and the nanocomposite with $\phi = 0.1$. We will come back to this issue when we will discuss Figure 4. In Figure 3b, we present the model predictions for the transient shear viscosity for two different values of the parameter x_{rel}: $x_{rel} = 0$ and $x_{rel} = 1$. A nonzero value for x_{rel} shifts the entire viscosity curve upward, and this is more pronounced for the smaller We values. Similar trends are observed in Figure 3c presenting the effect of κ' on the transient viscosity: a nonzero value for κ' (e.g., $\kappa' = 5\ \text{nm}^3$) shifts the viscosity curve slightly upward (especially at smaller We values). The most distinctive effect, however, is the appearance of the overshoot even for $We = 0.1$. The corresponding effect of the parameter Λ_0^{Ca} is illustrated in Figure 3(d): for $\Lambda_0^{Ca} = 0.1$, the entire viscosity curve is shifted slightly downward but its overall shape remains the same as when $\Lambda_0^{Ca} = 0$ [the case presented in Figure 3(c)].

The long-time asymptotic limits of the curves shown in Figure 3 define the corresponding steady-state shear viscosity values; their dependence on We (for several values of the important model parameters) is discussed in Figure 4. Part a of Figure 4 shows the comparison between the case with $\phi = 0$ (the neat polymer melt) and the cases with $\phi = 0.1$, $\phi = 0.2$, and $\phi = 0.3$. For $We = 0.1$, all curves approach the zero shear rate limit, in agreement with the analytic expression of eq 30a. As the value of We increases above ~0.1 and especially above ~1, shear thinning becomes pronounced. Interestingly enough, for $\Lambda_0^{Ca} = \kappa' = x_{rel} = 0$, the high shear rate asymptotic behavior of all curves in Figure 4a is the same. Figure 4b shows the effect of x_{rel} on viscosity: by increasing x_{rel}, the Newtonian plateau is shifted upward and the onset of shear thinning occurs at lower We values, but the high shear rate regime remains practically unaltered. It is only for a very large value of x_{rel} (e.g., $x_{rel} = 5$ in Figure 4b) that some differences can be detected in the high shear rate behavior of the nanocomposite. Exactly the same trends are observed when the value of κ' is increased (see Figure 4c). As far as the parameter Λ_0^{Ca} is concerned, Figure 4d shows that its effect is to shift the viscosity values in the Newtonian plateau downward without affecting the shear thinning behavior. The dependence of the model predictions for the shear viscosity on the molecular weight M_{mw} of the polymer is discussed in Figure 4e: increasing M_{mw} causes a slight increase of the viscosity in the Newtonian regime but apart from that the behavior at high We values remains unaltered. Finally, in Figure 4f, we show the effect of nanoparticle diameter D on viscosity: increasing D decreases the viscosity at low shear rates without significantly affecting the shear thinning behavior (at large We values).

B. Material Functions in Uniaxial Elongational Flow. Figure 5 illustrates the growth of the transient elongational viscosity in UEF for three different values of the dimensionless elongational rate We (now defined as $We = \lambda_0\dot{\varepsilon}_0$): $We = 0.1$, 1, and 10. First we compare the pure polymer to a nanocomposite containing 10% of nanoparticles (Figure 5a). For $We = 0.1$, the curve corresponding to the nanocomposite is above the one corresponding to the pure polymer; for $We = 1$, the opposite

dx.doi.org/10.1021/ma500415w | Macromolecules 2014, 47, 4493−4513

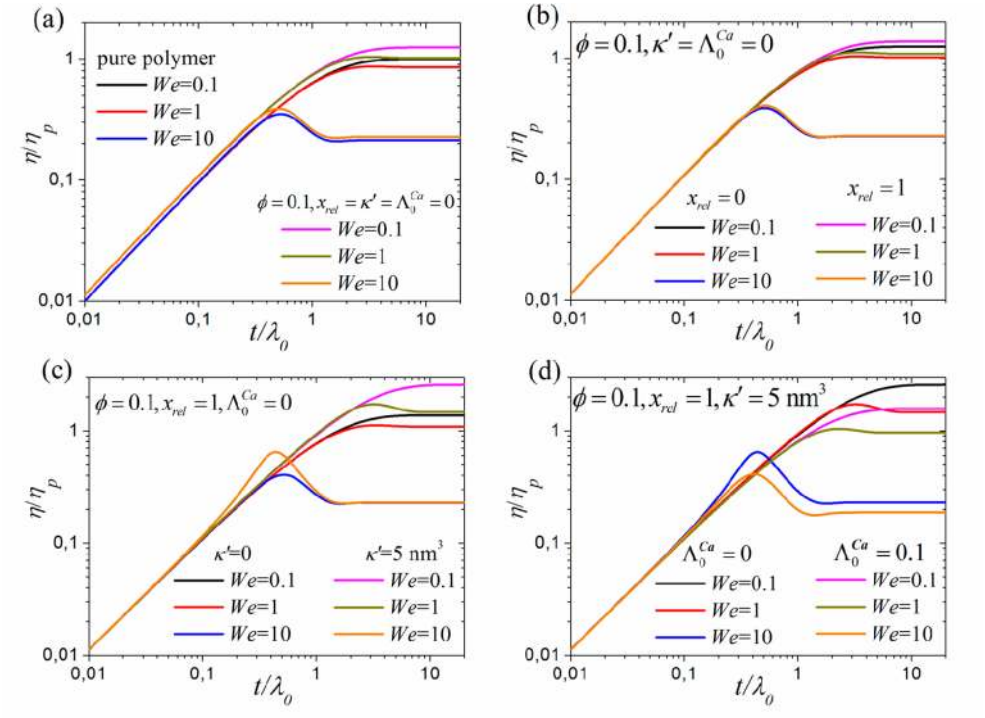

Figure 3. Model predictions for the growth (in time) of the relative viscosity η_r of the PNC for various values of the applied shear rate (or *We* number). Different sets of data are shown corresponding to different values of the set of model parameters $\{x_{rel}, \kappa', \Lambda_0^{Ca}\}$.

behavior is observed; and for *We* = 10, the two curves are seen to lie almost one on top of the other. This last feature is analogous to the results discussed in Figures 3 and 4 where upon increasing *We* the viscosity curve for the nanocomposite was found to approach that for the pure polymer. In Figure 5b, we present the viscosity curves for the nanocomposite for the case x_{rel} = 1: the curves are shifted upward but in a less pronounced way as the value of *We* is increased. And the same happens when κ' = 5 nm^3. Taking Λ_0^{Ca} = 0.1, on the other hand, causes the opposite effect, see Figure 5d: the viscosity curves are slightly shifted downward, similar to the behavior of the shear viscosity discussed in Figure 3d.

C. Conformation Tensor. The dependence of the most important elements ($\tilde{C}_{xx}$, $\tilde{C}_{yy}$, $\tilde{C}_{zz}$, and $\tilde{C}_{xy}$) of the conformation tensor $\tilde{\mathbf{C}}$ on *We* in the case of steady-state shear flow is examined in Figure 6. Several sets of curves are shown in the figure corresponding to different values of the set $\{x_{rel}, \kappa', \Lambda_0^{Ca}\}$, and they refer to a PNC with ϕ = 0.1 in addition to that for the pure polymer. For κ' = 0 (for which no swelling of polymer chains takes place), all diagonal elements of $\tilde{\mathbf{C}}$ start from the value of unity; in contrast, for $\kappa' > 0$, chains swell; in this case, the three diagonal elements of $\tilde{\mathbf{C}}$ start from values slightly larger than one. We also note that for Λ_0^{Ca} = 0 one can calculate analytically the asymptotic values of all four components $\tilde{C}_{xx}$, $\tilde{C}_{yy}$, $\tilde{C}_{zz}$, and $\tilde{C}_{xy}$ in the limit of infinitely high *We*, the resulting expressions being:

$$\frac{\tilde{C}_{yy}^{\infty}}{\tilde{C}_{xx}^{\infty}} = \frac{\xi}{2-\xi} \tag{33a}$$

$$\frac{\tilde{C}_{xx}^{\infty}}{\tilde{C}_{zz}^{\infty}} = \frac{2-\xi}{2\alpha_e}\left\{2\alpha_e - 1 + \sqrt{1 + \frac{4\alpha_e(1-\alpha_e)(1-\xi)^2}{\xi(2-\xi)}}\right\} \tag{33b}$$

$$\tilde{C}_{xx}^{\infty} = \frac{3}{2q(1-3\tilde{K})}\left\{b - 2 + q\frac{\tilde{C}_{xx}^{\infty}}{\tilde{C}_{zz}^{\infty}} - \tilde{K}b - \sqrt{\left[b - 2 + q\frac{\tilde{C}_{xx}^{\infty}}{\tilde{C}_{zz}^{\infty}} - \tilde{K}b\right]^2 - \frac{4}{3}(1-3\tilde{K})qb\frac{\tilde{C}_{xx}^{\infty}}{\tilde{C}_{zz}^{\infty}}}\right\} \tag{33c}$$

where $\alpha_e = \alpha(1-\xi)[1+f(\phi)]$, $\tilde{K} = 2/3n_a\kappa'[1+f(\phi)]^{-1}$ and $q = (\tilde{C}_{zz}^{\infty}/\tilde{C}_{xx}^{\infty}) + (2/\xi)(\tilde{C}_{yy}^{\infty}/\tilde{C}_{xx}^{\infty})$ (q is identical to ψ of ref 60; note also the correction to a typo to ψ in ref 60). Also shown in Figure 6 (by orange dotted lines) are the predictions of eq 31 for the asymptotic behavior of the four components in the limit of small *We*. The following conclusions can be drawn by inspecting the graphs of Figure 6:

- $\tilde{C}_{xx}$ increases monotonically with increasing *We* reaching a constant asymptotic value at *We* above approximately 200. Increasing the value of either x_{rel} or Λ_0^{Ca} shifts the curve at intermediate values of *We* upward and only slightly affects the value of the plateau in the limit of infinitely high shear rates. Compared to the pure polymer melt, polymer nanocomposites are characterized by relatively larger values of $\tilde{C}_{xx}$, especially for nonzero values of the parameter x_{rel}. Overall, $\tilde{C}_{xx}$ seems to be more sensitive to parameter x_{rel} than to parameters κ' and Λ_0^{Ca}. Keeping the values of x_{rel} and κ' fixed (equal to 5 and 1 nm^3, respectively), the asymptotic value of $\tilde{C}_{xx}$ for Λ_0^{Ca} = 0.1 is slightly below that for Λ_0^{Ca} = 0.
- $\tilde{C}_{yy}$ decreases monotonically with increasing *We* reaching an asymptotic value for *We* larger than ~200. This asymptotic value seems to be very small (equal to ~0.1) and practically insensitive to the exact values of the set $\{x_{rel}, \kappa', \Lambda_0^{Ca}\}$. We also observe that upon increasing the

dx.doi.org/10.1021/ma500415w | *Macromolecules* 2014, 47, 4493−4513

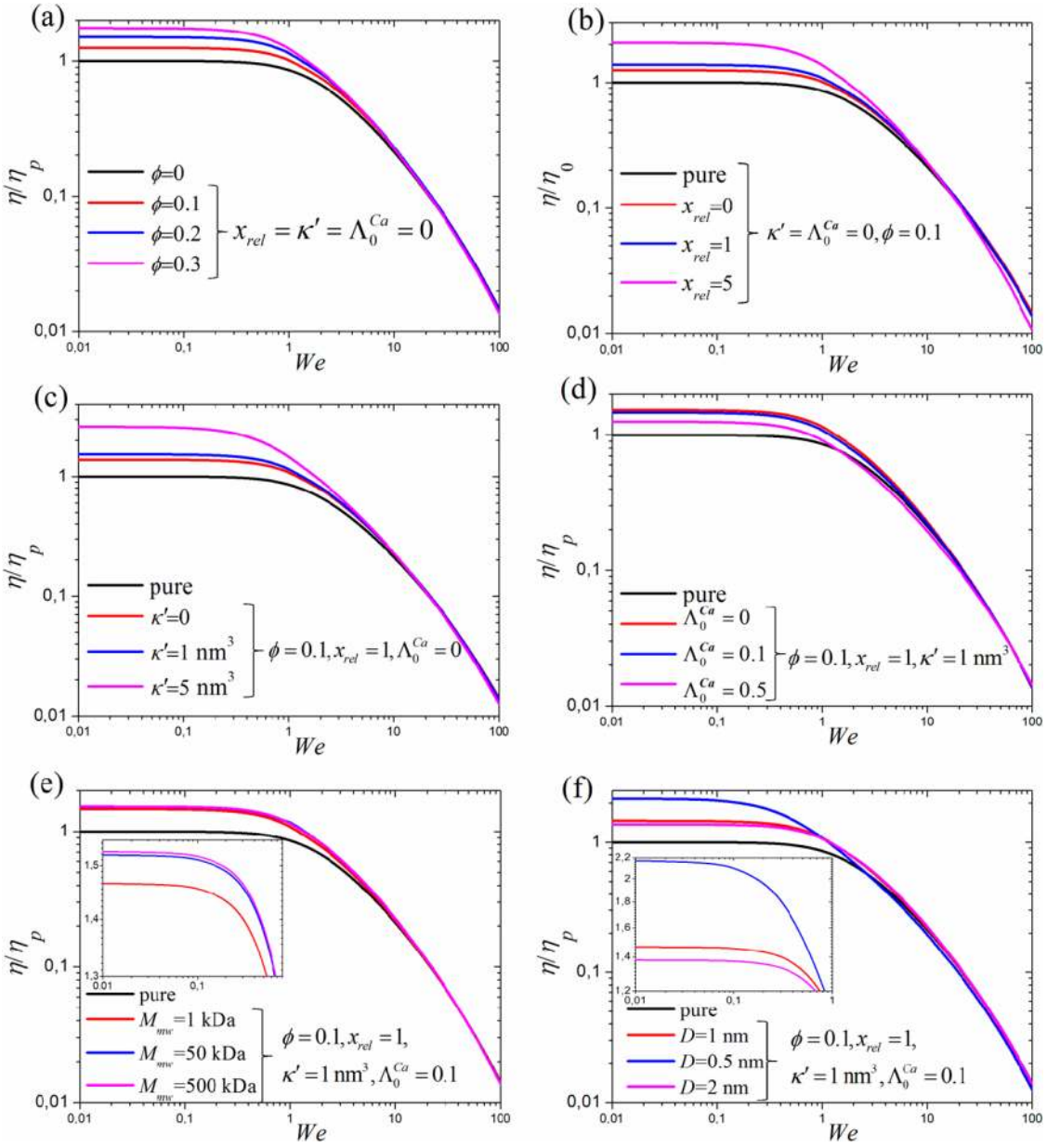

Figure 4. Model predictions for the variation of the relative zero shear rate viscosity of a PNC with shear rate (or *We* number). Different sets of data are shown corresponding to different values of the set of model parameters $\{x_{rel}, \kappa', \Lambda_0^{Ca}\}$.

value of x_{rel} the entire curve shifts downward (especially at intermediate *We*). Keeping the value of x_{rel} constant (e.g., equal to 5), increasing the values of κ' and Λ_0^{Ca} affects the behavior of the $\tilde{C}_{yy}$-vs-*We* curve only in the regime of small shear rates. Therefore, and similar to $\tilde{C}_{xx}$, $\tilde{C}_{yy}$ is more sensitive (overall) to parameter x_{rel} than to parameters κ' and Λ_0^{Ca}. We also see that PNCs are characterized by relatively smaller values of $\tilde{C}_{yy}$ (especially when x_{rel} attains nonzero values) compared to the corresponding pure polymer matrices. Keeping the values of x_{rel} and κ' fixed (equal to 5 and 1 nm^3, respectively), the asymptotic value of $\tilde{C}_{yy}$ for $\Lambda_0^{Ca} = 0.1$ is slightly below that for $\Lambda_0^{Ca} = 0$.

- Like $\tilde{C}_{yy}$, $\tilde{C}_{zz}$ decreases monotonically with *We* reaching also a constant asymptotic value at high enough *We* values (approximately above 200). However, and in contrast to $\tilde{C}_{yy}$, $\tilde{C}_{zz}$ undergoes a smaller variation with *We*. For example, its asymptotic value (in the limit of infinitely high shear rates) is always larger than 0.5. We also find that this asymptotic value depends strongly on the value of Λ_0^{Ca}: increasing Λ_0^{Ca}, causes the entire $\tilde{C}_{zz}$-vs-*We* curve to shift upward. The parameter κ', on the other hand, seems to affect the variation of $\tilde{C}_{zz}$ with shear rate only in the regime of small *We*.
- In contrast to the three diagonal elements ($\tilde{C}_{xx}$,$\tilde{C}_{yy}$, and $\tilde{C}_{zz}$), the nondiagonal $\tilde{C}_{xy}$ element of $\tilde{\mathbf{C}}$ changes with *We* in a nonmonotonic way: with increasing *We*, its value initially increases, goes through a maximum at an intermediate *We* value, and then drops rapidly. The maximum value of $\tilde{C}_{xy}$ is slightly above 1 and is attained for a value of *We* that depends slightly on the exact values of the parameters x_{rel}, κ', and Λ_0^{Ca} (in all cases, it is close to 100).

dx.doi.org/10.1021/ma500415w | *Macromolecules* 2014, 47, 4493−4513

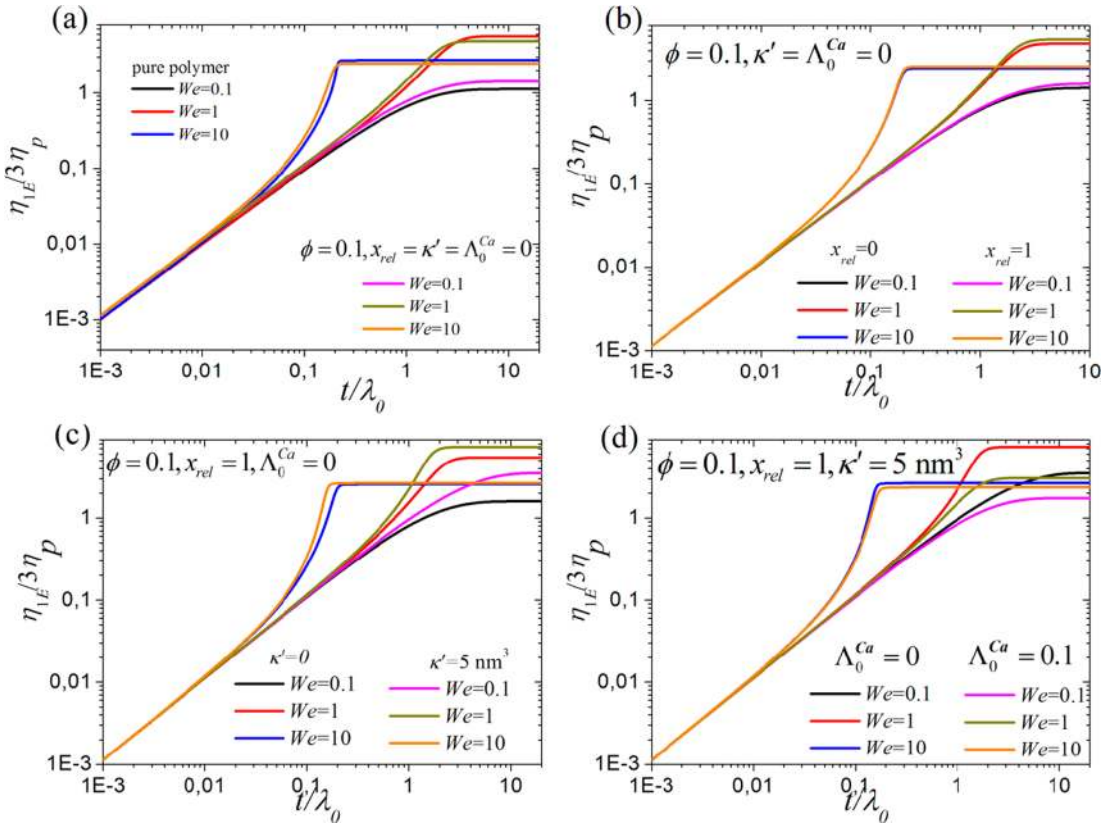

Figure 5. Same as with Figure 3 but for the uniaxial elongational viscosity (in scaled units).

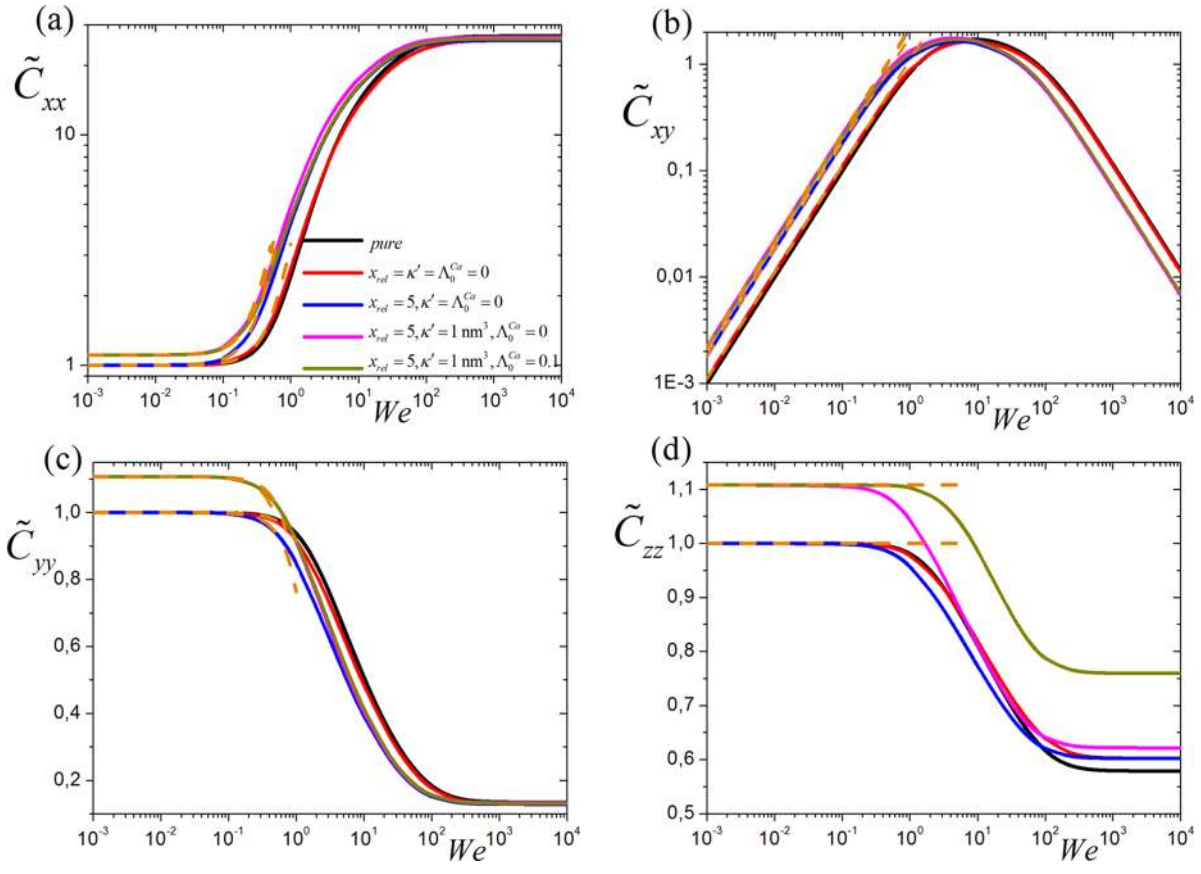

Figure 6. Model predictions for the components of the conformation tensor for different values of the set of model parameters $\{x_{rel}, \kappa', \Lambda_0^{Ca}\}$. Similar to Figure 4, we have used that $f(\phi) = (5/2)\phi$.

dx.doi.org/10.1021/ma500415w | *Macromolecules* 2014, 47, 4493−4513

D. Comparison with Experimental Data. The capability of our model to describe quite accurately experimentally measured data for several nanocomposite melts is demonstrated in Figures 7 and 8. Figure 7 shows how well the new

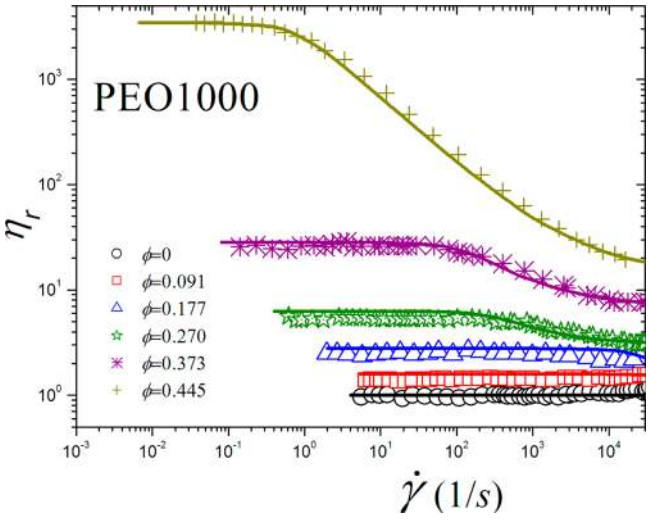

Figure 7. Comparison of model predictions for the relative viscosity of a PNC as a function of nanoparticle volume fraction and imposed shear with the experimental measurements of Anderson and Zukoski.[43]

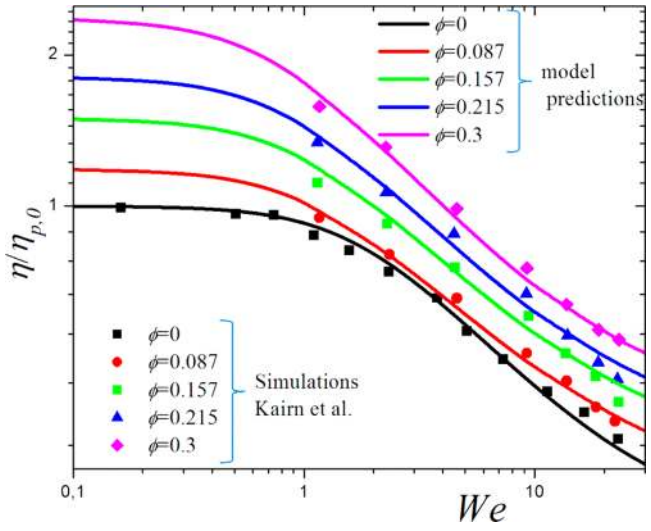

Figure 8. Same as with Figure 6 but with the simulation data of Kairn et al.[22]

model can describe the relative viscosity of an unentangled PEO melt with molecular weight M_{mw} = 1000 g/mol filled with silica nanoparticles of diameter D = 43 nm.[43] The pure polymer exhibits a constant viscosity with shear rate suggesting the following values for the pure polymer parameters: $\xi = \alpha = \varepsilon = 0$ and $b \to \infty$ (i.e., Hookean dumbbells), see also Stephanou et al.[69] Furthermore, due to the large nanoparticle volume fractions covered in the measurements (close to 50%), neither the Einstein equation nor the Einstein–Berthelot–Green one are applicable.[43] A better choice is the empirical equation proposed by Krieger–Dougherty[75] for dense Newtonian suspensions with ϕ_T denoting the value of the maximum packing fraction. We also observe that for $\phi \geq 0.27$ the data in Figure 7 exhibit a plateau in the limit of infinitely high shear rates. This is due to the fact that, at these high shear rates, flow is so fast that thermal motion cannot destroy the imposed structure (fully aligned molecules) on polymer chains. Inspired by the Carreau–Yasuda model,[78] such a behavior in our work is captured by using $[\eta - \eta_\infty(\phi)]/[\eta_0(\phi) - \eta_\infty(\phi)] = \tau_{xy}/[\eta_0(\phi)\dot{\gamma}_0]$ which for $We \ll 1$ approaches unity so that $\eta = \eta_0(\phi)$ while for $We \gg 1$ we obtain $\eta = \eta_\infty(\phi)$ (i.e, the infinite shear rate viscosity). Using then $\phi_T^{-1} = 2.242$, $\kappa' = 10^3$ nm^3 and $x_{rel} = 4.4$, our model offers a very satisfactory description of the experimental data provided that a ϕ-dependent value is used for Λ_0^{Ca}. The corresponding results are shown in Figure 7 and have been obtained with the following best-fit values for Λ_0^{Ca}: $\Lambda_0^{Ca} = 10^{-11}$ for $\phi = 0.091$, $\Lambda_0^{Ca} = 7 \times 10^{-11}$ for $\phi = 0.177$, $\Lambda_0^{Ca} = 3 \times 10^{-7}$ for $\phi = 0.27$, $\Lambda_0^{Ca} = 5 \times 10^{-7}$ for $\phi = 0.373$, and $\Lambda_0^{Ca} = 3 \times 10^{-2}$ for $\phi = 0.445$; also, $\eta_\infty(\phi = 0.445) = 15$, $\eta_\infty(\phi = 0.373) = 7$, and $\eta_\infty(\phi = 0.27) = 3$ (in units of η_0). The best-fit value of κ' ($= 10^3$ nm^3) is very close to the one calculated by eq 31 which gives $\kappa' \approx 6 \times 10^3$ nm^3 (the bead size has been obtained via $b_d^2 = m_0(\langle R_{ete}^2\rangle_{eq}/M_{mw})$ where $m_0 = 44$ g/mol for PEO). We further note that the equilibrium relaxation time of the pure polymer comes out to be $\lambda_0 = 0.15$ s. A similar calculation for PEO400[68] gives $\lambda_0 = 8 \times 10^{-3}$ s. Combining the two sets of data suggests a scaling of the form $\lambda_0 \sim M_{mw}^{1.76}$, which does not deviate much from the scaling $\lambda_0 \sim M_{mw}^2$ proposed by the combined Rouse-free volume theory.[79] Overall, our model provides a very good description of the nonlinear rheological properties of the PEO-silica nanocomposites studied by Anderson and Zukoski[43] over a very large range of shear rates, irrespective of the nanoparticle volume fraction ϕ used in the rheological measurements. An interesting observation is that the fitted η_∞ values are not only in excellent agreement with those reported by Anderson–Zukoski (ref 43, Figure 4B) but also fully compatible with the expression $\eta_\infty(\phi) \approx (1 - y\phi)^{-2}$ with $y \approx 1.66$ proposed on the basis of a large amount of literature data on monodisperse spheres.[80]

Figure 8 presents a further comparison of our model with the coarse-grained NEMD simulation predictions of Kairn et al.[22] The data refer to an unentangled polypropylene melt with chain molecular weight M_{mw} = 2200 g/mol filled with nanoparticles interacting with a modified WCA potential with D = 1.55 nm. Here, the pure polymer melt exhibits shear-thinning, and this is captured by using the following set of parameters: $\alpha = \xi = 0.01$, $\varepsilon = 0.02$, and $b = 36.6$. Actually, the value of b was not fitted but was directly obtained from $b = 3L_c^2/\langle R_{ete}^2\rangle_{eq}$ by using $L_c = 19$ and $\langle R_{ete}^2\rangle_{eq} = 29.5$ (in units of σ and σ^2, respectively).[22] For the function f we made use of the Einstein-Berthelot-Green expression (as suggested by Kairn et al.), namely $f(\phi) = 2.5\phi + 6.2\phi^2$. The best fits to the simulation data were then obtained for $\Lambda_0^{Ca} = 1$, $x_{rel} = 0.3$ and $\kappa' = 1$ nm^3. As far as the infinite shear rate viscosity values are concerned, these came out to be: $\eta_\infty(\phi = 0.3) = 0.4$, $\eta_\infty(\phi = 0.215) = 0.36$, $\eta_\infty(\phi = 0.157) = 0.33$, $\eta_\infty(\phi = 0.087) = 0.28$, and $\eta_\infty(\phi = 0) = 0.23$ (in units of $\eta_p = (1-\xi)^2\eta_0$). The curves shown in Figure 8, then give a picture of the accuracy that the model can reproduce the simulation data.

VI. DISCUSSION AND CONCLUSIONS

A constitutive model has been introduced for the thermodynamics and hydrodynamics of polymer nanocomposite melts at a mesoscopic level of description, capable of providing a very accurate and self-consistent picture of many important properties of this class of materials. The model has been developed in the framework of the generalized bracket and

dx.doi.org/10.1021/ma500415w | Macromolecules 2014, 47, 4493–4513

GENERIC formalisms of nonequilibrium thermodynamics and leads to a set of time evolution equations for the important transport processes and their couplings in polymer nanocomposites, nicely extending previous approaches developed for simpler systems, such as a Newtonian suspension of particles or a pure homopolymer melt. The proposed model has several attractive features: (a) it is based on a few fundamental building blocks that have either a clear physical meaning (such as the terms in the Helmholtz free energy describing polymer−nanoparticle interactions) or a strict mathematical structure (such as the Poisson and the dissipative brackets); (b) the formulation in terms of thermodynamic quantities (such as an extended free energy) allows for the consistent extension of equilibrium theoretical approaches to nonequilibrium conditions; (c) the building blocks are put together in a form allowing for the smooth incorporation into the model of new physics coming from more detailed approaches (such as atomistic simulations) or more fundamental theories (e.g., kinetic theory for the description of the most important hydrodynamic interactions); (d) the model obeys the first and second law of thermodynamics, which poses important constraints on its parameters; (e) there is a clear correspondence of all terms in the evolution equations to an underlying molecular mechanism or phenomenon (this adds extra power to its predictive capability); (f) the final equations provide a clear description of the coupling between microstructure, thermodynamics and transport properties; (g) for simpler systems, the proposed set of dynamic equations correctly reduces to known (and well-tested) models.

Overall, the proposed model offers a unified description of several aspects of PNCs: it can describe their phase behavior (miscibility), conformational properties (degree of chain swelling due to nanoparticles), zero shear rate viscosity and dependence on nanoparticle volume fraction and size, and all rheological material functions in shear and elongation (including the dependence on nanoparticle volume fraction and deformation rate).

The new model has been validated by showing how it can describe (fit) several sets of thermodynamic and rheological data reported in the literature either from direct experimental measurements or from simulations. For example, the model can provide a very reliable description of the experimental measurements of Anderson and Zukoski[43] for the dependence of viscosity on nanoparticle volume fraction both in the Newtonian plateau and in the shear thinning regime. This was also true with the corresponding simulation data of Kairn et al.[22] Moreover, the model can describe very satisfactorily the experimental result of Mackay et al.[40] for the dependence of chain swelling on nanoparticle volume fraction in several polystyrene-based nanocomposites.[69]

As a continuation of the present work, we would like to (a) introduce strategies for estimating most (if not all) of the model parameters from lower-level studies (e.g., from detailed molecular simulations), (b) extend the model to entangled polymers, and (c) use the new model to study how the applied flow can affect the phase behavior of the polymer nanocomposite.

APPENDIX A

A Quick Overview of Flory−Huggins Theory

According to the Flory−Huggins theory (Flory,[81] Chapter XII):

$$\frac{\Delta A}{Vk_BT} = n_p \ln(1-\phi) + n_a[\ln\phi + \chi(1-\phi)] \tag{A1}$$

where n_a and n_p denote the polymer chain density and nanoparticle number density, respectively, χ the Flory−Huggins mixing parameter, and V the volume of the specimen. Equation A1 can also be written as

$$\frac{\Delta A}{Vk_BT} = \frac{\rho_p N_{av}}{M_{mw}}(1-\phi)\ln(1-\phi) + \frac{1}{\nu_{np}}[\phi\ln\phi + \chi\phi(1-\phi)] \tag{A2}$$

By further multiplying with the nanoparticle volume ν_{np} we get

$$\frac{\nu_{np}\Delta A}{Vk_BT} = \frac{\nu_{np}\rho_p N_{av}}{M_{mw}}(1-\phi)\ln(1-\phi) + \phi\ln\phi + \chi\phi(1-\phi) \tag{A3}$$

Following Mackay et al.,[40] we can introduce next the parameter $t_M = \nu_{np}\rho_p N_{av}/M_{mw}$, which can also be written as

$$t_M = \frac{\nu_{np}\rho_p N_{av}}{M_{mw}} = \left(\frac{4}{3}\pi a^3\right)\rho_p \frac{1}{\rho_0\left(\frac{4}{3}\pi R_{g0}^3\right)} = \left(\frac{D}{2R_{g0}}\right)^3 \frac{\rho_p}{\rho_0} \tag{A4}$$

where a denotes the radius of the nanoparticles, ρ_0 is the density of one chain, and R_{g0} is the radius-of-gyration of the polymer chains in the pure polymer state. An alternative expression in terms of the polymer molecular weight $M_{mw} = m_1 N_{av} N$, where N is the polymerization and m_1 the mass of one monomer, and the density of the pure polymer $\rho_p = m/V = N_p N m_1/N_p N v_1 = m_1/v_1$ ($v_1 = 4/3\pi b_d^3$ is the volume occupied by one monomer) is

$$t_M = \frac{\nu_{np}\rho_p N_{av}}{M_{mw}} = \nu_{np}\frac{m_1}{v_1}\frac{N_{av}}{m_1 N_{av} N} = \frac{\nu_{np}}{v_1}\frac{1}{N} \tag{A5}$$

APPENDIX B

Finite Nonlinear Chain Extensibility

We focus on the definition of the chain extensibility parameter μ introduced by Stephanou et al.[60] (their eq 19):

$$\mu^2 = \frac{\langle R_{ete}^2\rangle - \langle R_{ete}^2\rangle_{eq}^0}{L_c^2 - \langle R_{ete}^2\rangle_{eq}^0} \tag{B1}$$

It should be noted that the reference state is again[60,61] the pure polymer one. The parameter μ^2 can be cast in terms of dimensionless quantities by multiplying and dividing with K/k_BT:

$$\mu^2 = \frac{1}{b-3}\mathrm{tr}(\tilde{\mathbf{C}} - \mathbf{I}) \tag{B2}$$

For a pure polymer and under equilibrium conditions (i.e., for $\tilde{\mathbf{C}} = \mathbf{I}$), $\mu^2 = 0$. The effective spring constant defined as (the correction in eq (5a) of Stephanou et al.[60] should be noted)

$$h(\mathrm{tr}\,\mathbf{C}) = 2\frac{\delta A}{\delta \mathrm{tr}\,\mathbf{C}} = \frac{\partial\Phi}{\partial \mathrm{tr}\,\mathbf{C}} = \frac{K}{k_BT}\frac{\partial\Phi}{\partial \mathrm{tr}\,\tilde{\mathbf{C}}} \tag{B3}$$

is thus given by

$$h^W(\mathrm{tr}\,\mathbf{C}) = \frac{1}{1-\mu^2} = \frac{1}{1-\frac{1}{b-3}\mathrm{tr}(\tilde{\mathbf{C}}-\mathbf{I})} = \frac{b-3}{b-\mathrm{tr}\,\tilde{\mathbf{C}}} \tag{B4}$$

$$h^C(\mathrm{tr}\,\mathbf{C}) = \frac{1}{3}\frac{3-\mu^2}{1-\mu^2} = \frac{1}{3}\frac{3-\frac{1}{b-3}\mathrm{tr}(\tilde{\mathbf{C}}-\mathbf{I})}{1-\frac{1}{b-3}\mathrm{tr}(\tilde{\mathbf{C}}-\mathbf{I})} = \frac{1}{3}\frac{3(b-2)-\mathrm{tr}\,\tilde{\mathbf{C}}}{b-\mathrm{tr}\,\tilde{\mathbf{C}}} \tag{B5}$$

for the FENE-P(Warner) approximation and the FENE-P(Cohen) approximation, respectively. We note that, contrary to the case discussed in Stephanou et al.,[60,61] the effective spring constant at equilibrium does *not* reduce to unity unless chains are very long ($b \gg 1$). Equations B4 and B5 are obtained from eq B3 by assuming the following expressions, respectively, for the potential energy:

$$\Phi^W = -(L_c^2 - \langle R_{\mathrm{ete}}^2\rangle_{\mathrm{eq}}^0)\ln\left(1-\frac{\mathrm{tr}\left(\mathbf{C}-\frac{k_BT}{K}\mathbf{I}\right)}{L_c^2-\langle R_{\mathrm{ete}}^2\rangle_{\mathrm{eq}}^0}\right) = -\frac{k_BT}{K}(b-3)\ln\left(1-\frac{\mathrm{tr}(\tilde{\mathbf{C}}-\mathbf{I})}{b-3}\right)$$

$$\Phi^C = \frac{1}{3}\left[\mathrm{tr}\left(\mathbf{C}-\frac{k_BT}{K}\mathbf{I}\right) - 2(L_c^2-\langle R_{\mathrm{ete}}^2\rangle_{\mathrm{eq}}^0)\times\ln\left(1-\frac{\mathrm{tr}\left(\mathbf{C}-\frac{k_BT}{K}\mathbf{I}\right)}{L_c^2-\langle R_{\mathrm{ete}}^2\rangle_{\mathrm{eq}}^0}\right)\right] = \frac{k_BT}{3K}\left[\mathrm{tr}(\tilde{\mathbf{C}}-\mathbf{I}) - 2(b-3)\ln\left(1-\frac{\mathrm{tr}(\tilde{\mathbf{C}}-\mathbf{I})}{b-3}\right)\right] \tag{B6}$$

It should be noted that the correct form of eq (23a) in Stephanou et al.[60] is (in their notation):

$$\phi^W = -(b-3)\ln\left(1-\frac{\mathrm{tr}(\tilde{\mathbf{C}}-\mathbf{I})}{b-3}\right) \tag{B7a}$$

Although eqs B7a and eq 23a in Stephanou et al.[60] both give the same effective spring constant, eq 21, only eq B7a gives $\phi^W = \mathrm{tr}(\tilde{\mathbf{C}}-\mathbf{I})$, which vanishes at equilibrium; in contrast, eq 23a in Stephanou et al.[60] gives $\phi^W = \mathrm{tr}\,\tilde{\mathbf{C}}$, which does not vanish at equilibrium. Equation 23b in Stephanou et al.[60] may be rewritten as

$$\phi^C = \left[\mathrm{tr}(\tilde{\mathbf{C}}-I) - 2(b-3)\ln\left(1-\frac{\mathrm{tr}(\tilde{\mathbf{C}}-I)}{b-3}\right)\right] \tag{B7b}$$

Equations B7a and B7b agree with eqs B6 by taking $K\Phi^j/k_BT = \phi^j$, $j=\{W,C\}$.

APPENDIX C

Rotational Relaxation Time of a Spheroid and Its Dependence on Volume Fraction

We first consider the case of a pure unentangled polymer melt at equilibrium whose viscosity η_p is typically given in terms of its number density n_p and chain longest relaxation time λ_0 through

$$\eta_p = n_pk_BT\lambda_0 \Rightarrow \lambda_0 = \frac{\eta_p}{n_pk_BT} \tag{C1}$$

The volume fraction of the particle is $\phi = v_{\mathrm{np}}/V$, where v_{np} denotes the volume of the particle and V the volume of the specimen. Since only one particle has been added, the volume is considered to remain unchanged (equal to that of the pure polymer), namely $V = m/\rho = M_{\mathrm{mv}}/(N_{\mathrm{av}}\rho) = (n_p)^{-1}$, thus $v_{\mathrm{np}} = \phi/n_p$. The rotational friction coefficient for a prolate ellipsoid is $\zeta_r \sim \eta_pL_a^3$, where L_a is the length of the long axis (actually, the expression is more complex and contains also the prolate ellipsoid's aspect ratio; see Jeffery[28] and Doi and Edwards,[79] p 292). The rotational diffusion coefficient is therefore $D_r = k_BT/\zeta_r$, implying that the characteristic time needed for the particle to complete one full rotation is

$$\lambda_a \sim (D_r)^{-1} \sim \frac{\eta_pL_a^3}{k_BT} \tag{C2}$$

Note that in the case of a sphere $\zeta_r \sim \eta_pD^3$ and $\lambda_a \sim \eta_pL_a^3/(k_BT)$; the latter agrees with the rotation time given by Tanford[82] (reference available in Doi and Edwards[79] p. 103, eq 4.83). Since only one particle has been inserted, we can take the polymer viscosity and the polymer chain radius-of-gyration to be constant (but we will revisit this below); by combining then the above equations, we get

$$\lambda_a \sim \frac{\eta_pL_a^3}{k_BT} \sim n_p\lambda_0L_a^3 \sim \phi\lambda_0\frac{L_a^3}{v_{np}} \tag{C3}$$

In the case of a sphere $v_{\mathrm{np}} \sim L_a^3 = D^3$. This shows that for very dilute suspensions the rotational relaxation time of the nanoparticles is proportional to $\phi\lambda_0$.

Let us consider now the case where the viscosity of the suspension follows Einstein's law $\eta_p(\phi) = \eta_p(1+c_1\phi)$. As we add nanoparticles to the matrix, the polymer number density will decrease according to $n_p(\phi) = (1-\phi)N_{\mathrm{av}}\rho/M_{\mathrm{mw}} = (1-\phi)n_p$. Combining the two expressions, we see that

$$\lambda_a \sim \frac{\eta_p(1+c_1\phi)L_a^3}{k_BT} \sim (1+c_1\phi)(1-\phi)n_p\lambda_0L_a^3 \sim (1+c_1\phi)(1-\phi)\phi\lambda_0\frac{L_a^3}{v_{\mathrm{np}}} \tag{C4}$$

But ϕ is negligibly small, thus again $\lambda_a \sim \phi\lambda_0(L_a^3/v_{\mathrm{np}})$.

ASSOCIATED CONTENT

Supporting Information

Volterra derivatives of the free energy, thermodynamic admissibility and positive semi-definiteness of the conformation tensor, GENERIC derivation of the model, and derivation of a relation for the parameter κ'. This material is available free of charge via the Internet at http://pubs.acs.org.

AUTHOR INFORMATION

Corresponding Author

*Telephone: +357 22 893916. Fax: +357 22 892601. E-mail: stephanou.pavlos@ucy.ac.cy (P.S.S.).

Notes

The authors declare no competing financial interest.

■ ACKNOWLEDGMENTS

P.S.S. would like to dedicate this work to his firstborn son (June 2nd) Michael. This work was cofunded by the European Regional Development Fund and the Republic of Cyprus through the Research Promotion Foundation (Project: DIDAKTOR/0311/40) (PSS).

■ REFERENCES

(1) Currey, J. D. In *Handbook of composites-Fabrication of composites*; Kelly, A., Mileiko, S. T., Eds.; Elsevier: New York, 1983; Vol. *4*, pp 501−564.
(2) Koo, J. H. *Polymer Nanocomposites: Processing, characterization and applications*, 1st ed.; McGraw-Hill Professional: New York, 2006.
(3) Oriakhi, C. O. *J. Chem. Educ.* **2000**, *77*, 1138−1146.
(4) Larson, R. G. *The structure and rheology of complex fluids*; Oxford University Press: New York, 1999.
(5) Moulé, A. J.; Allard, S.; Kronenberg, N. M.; Tsami, A.; Scherg, U.; Meerholz, K. *J. Phys. Chem. C. Lett.* **2008**, *112*, 12583−12589. Jancar, J.; Douglas, J. F.; Starr, F. W.; Kumar, S. K.; Cassagnau, P.; Lesser, A. J.; Sternstein, S. S.; Buehler, M. J. *Polymer* **2010**, *51*, 3321−3343.
(6) Kumar, S. K.; Krishnamoorti, R. *Annu. Rev. Chem. Biomol. Eng.* **2010**, *1*, 37−58.
(7) Salata, O. V. *J. Nanobiotechnol.* **2004**, *2*, 3. Feifel, S. C.; Lisdat, F. *J. Nanobiotechnology* **2011**, *9*, 59.
(8) Vaia, R. A.; Maguire, J. F. *Chem. Mater.* **2007**, *19*, 2736−2751.
(9) Ke, Y. C.; Stroeve, P. *Polymer-Layered Silicate and Silica Nanocomposites*; Elsevier B.V.: Amsterdam, 2005.
(10) Mittal, V. *Materials* **2009**, *2*, 992−1057.
(11) Zou, H.; Wu, S.; Shen, J. *Chem. Rev.* **2008**, *108*, 3893−3957.
(12) Moniruzzaman, M.; Winey, K. I. *Macromolecules* **2006**, *39*, 5194−5205.
(13) Morgan, P. *Carbon Fibers and Their Composites*; Taylor and Francis Group, CRC: Boca Raton, FL, 2005.
(14) Zeng, Q. H.; Yu, A. B.; Lu, G. Q. *Prog. Polym. Sci.* **2008**, *33*, 191−269. Liu, J.; Zhang, L.; Cao, D.; Wang, W. *Phys. Chem. Chem. Phys.* **2009**, *11*, 11365−11384. Pandey, Y. N.; Papakonstantopoulos, G. J.; Doxastakis, M. *Macromolecules* **2013**, *46*, 5097−5106.
(15) Liu, J.; Cao, D.; Zhang, L.; Wang, W. *Macromolecules* **2009**, *42*, 2831−2842.
(16) Allegra, G.; Raos, G.; Vacatello, M. *Prog. Polym. Sci.* **2008**, *33*, 683−731. Hall, L. M.; Jayaraman, A.; Schweizer, K. S. *Curr. Opin. Colloid Interface Sci.* **2010**, *14*, 38−48.
(17) Solomon, M. J.; Lu, Q. *Curr. Opin. Colloid Interface Sci.* **2001**, *6*, 430−437. Schmidt, G.; Malwitz, M. M. *Curr. Opin. Colloid Interface Sci.* **2003**, *8*, 103−108.
(18) Vacatello, M. *Macromolecules* **2002**, *35*, 8191−8193. Vacatello, M. *Macromol. Theory Simul.* **2002**, *11*, 757−765. Vacatello, M. *Macromol. Theory Simul.* **2003**, *12*, 86−91.
(19) Dionne, P. J.; Ozisik, R.; Picu, C. R. *Macromolecules* **2005**, *38*, 9351−9358.
(20) Vladkov, M.; Barrat, J.-L. *Macromolecules* **2007**, *40*, 3797−3804. Toepperwein, G. N.; Karayiannis, N.Ch.; Riggleman, R. A.; Kröger, M.; de Pablo, J. J. *Macromolecules* **2011**, *44*, 1034−1045.
(21) Li, Y.; Kröger, M.; Liu, W. K. *Macromolecules* **2012**, *45*, 2099−2112.
(22) Kairn, T.; Daivis, P. J.; Ivanov, I.; Bhattacharya, S. N. *J. Chem. Phys.* **2005**, *123*, 194905.
(23) Smith, G. D.; Bedrov, D.; Li, L.; Byutner, O. *J. Chem. Phys.* **2002**, *117*, 9478−9489. Pryamitsyn, V.; Ganesan, V. *Macromolecules* **2006**, *39*, 844−856. Knauert, S. T.; Douglas, J. F.; Starr, F. W. *J. Polym. Sci., Part B: Polym. Phys.* **2007**, *45*, 1882−1897. Thomin, J. D.; Keblinski, P.; Kumar, S. K. *Macromolecules* **2007**, *41*, 5988−5991.
(24) Starr, F. W.; Douglas, J. F.; Glotzer, S. C. *J. Chem. Phys.* **2003**, *119*, 1777−1788.
(25) Einstein, A. *Ann. Phys.* **1906**, *19*, 289−306; *Ann. Phys.* **1911**, *34*, 591−592. Einstein, A. *Investigations on the theory of Brownian Movement*; Dover Publications Inc.: London, 1956.
(26) Batchelor, G. K.; Green, J. T. *J. Fluid Mech.* **1972**, *56*, 375−400 *ibid*, 401−427; **1972**, *56*, 401−427.
(27) Litchfield, D. W.; Baird, D. G. *Rheol. Rev.* **2006**, 1−60. Mueller, S. E.; Llewellin, W. H.; Mader, M. *Proc. R. Soc. London, A* **2010**, *466*, 1201−1228.
(28) Jeffery, G. B. *Proc. R. Soc. London, A* **1922**, *102*, 161−179.
(29) Hinch, E. J.; Leal, L. G. *J. Fluid Mech.* **1972**, *52*, 683−712. Leal, L. G.; Hinch, E. J. *J. Fluid Mech.* **1971**, *46*, 685−703.
(30) Batchelor, G. K. *J. Fluid Mech.* **1970**, *41*, 545−570. Brenner, H. *Chem. Eng. Sci.* **1972**, *27*, 1069−1107.
(31) Dörr, A.; Sadiki, A.; Mehdizadeh, A. *J. Rheol.* **2013**, *57*, 743−765.
(32) Metzner, A. B. *J. Rheol.* **1985**, *29*, 739−775.
(33) Tuteja, A.; Mackay, M. E.; Hawker, C. J.; Van Horn, B. *Macromolecules* **2005**, *38*, 8000−8011. Mackay, M. E.; Dao, T. T.; Tuteja, A.; Ho, D. L.; Van Horn, B.; Kim, H.-C.; Hawker, G. J. *Nat. Mater.* **2003**, *2*, 762−766.
(34) Jain, S.; Goossens, J. G. P.; Peters, G. W. M.; van Duin, M.; Lemstra, P. J. *Soft Matter* **2008**, *4*, 1848−1854.
(35) Wang, M.; Hill, R. J. *Soft Matter* **2009**, *5*, 3940−3953.
(36) Starr, F. W.; Schrøder, T. B.; Glotzer, S. C. *Phys. Rev. E* **2001**, *64*, 021802. Starr, F. W.; Schrøder, T. B.; Glotzer, S. C. *Macromolecules* **2002**, *35*, 4481−4492.
(37) Anastassiou, A. *Structure-property (viscoelastic, mechanical, and adhesive) relationships in poly-acrylic adhesives through atomistic simulations*, Ph.D. Thesis, University of Patras: Patras, Greece, 2013.
(38) Hooper, J. B.; Schweizer, K. S. *Macromolecules* **2006**, *39*, 5133−5142.
(39) Liu, J.; Gao, Y.; Cao, D.; Zhang, L.; Guo, Z. *Langmuir* **2011**, *27*, 7926−7933.
(40) Mackay, M. E.; Tuteja, A.; Duxbury, P. M.; Hawker, C. J.; Van Horn, B.; Guan, Z.; Chen, G.; Kishnan, R. S. *Science* **2006**, *311*, 1740−1743.
(41) Tuteja, A.; Duxbury, P. M.; Mackay, M. E. *Phys. Rev. Lett.* **2008**, *100*, 077801.
(42) Crawford, M. K.; Smalley, R. J.; Cohen, G.; Hogan, B.; Wood, B.; Kumar, S. K.; Melnichenko, Y. B.; He, L.; Guise, W.; Hammouda, B. *Phys. Rev. Lett.* **2013**, *110*, 196001.
(43) Anderson, B. J.; Zukoski, C. F. *Macromolecules* **2008**, *41*, 9326−9334.
(44) Anderson, B. J.; Zukoski, C. F. *Macromolecules* **2009**, *42*, 8370−8384. Anderson, B. J.; Zukoski, C. F. *Langmuir* **2010**, *26*, 8709−8720.
(45) Zhang, Q.; Archer, L. A. *Macromolecules* **2004**, *37*, 1928−1936.
(46) Rajabian, M.; Naderi, G.; Dubois, C.; Lafleur, P. G. *Rheol. Acta* **2010**, *49*, 105−118.
(47) Rajabian, M.; Dubois, C.; Grmela, M. *Rheol. Acta* **2005**, *44*, 521−535. Rajabian, M.; Dubois, C.; Grmela, M.; Carreau, P. J. *Rheol. Acta* **2008**, *47*, 701−717.
(48) Bird, R. B.; Curtiss, C. F.; Armstrong, R. C.; Hassager, O. *Dynamics of Polymeric Liquids; Vol. 2, Kinetic Theory*, 2nd ed.; John Wiley and Sons: New York, 1987.
(49) Doremus, P.; Piau, J. M. *J. Non-Newtonian Fluid Mech.* **1991**, *39*, 335−352.
(50) Havet, G.; Isayev, A. I. *Rheol. Acta* **2001**, *40*, 570−581.
(51) Sarvestani, A. S.; Picu, C. R. *Polymer* **2004**, *45*, 7779−7790. Sarvestani, A. S.; Picu, C. R. *Rheol. Acta* **2005**, *45*, 132−141.
(52) Xu, J.; Chatterjee, S.; Koelling, K. W.; Wang, Y.; Bechetel, S. E. *Rheol. Acta* **2005**, *44*, 537−562.
(53) Sarvestani, A. S.; Jabbari, E. *Macromol. Theory Sim.* **2007**, *16*, 378−385. Kalfus, J.; Jancar, J. *J. Polym. Sci., Part B: Polym. Phys.* **2007**, *45*, 1380−1388. Sarvestani, A. S. *Eur. Polym. J.* **2008**, *44*, 263−269. Kabanemi, K. K.; Hetu, J.-F. *J. Non-Newtonian Fluid Mech* **2010**, *165*, 866−878.
(54) Grmela, M.; Öttinger, H. C. *Phys. Rev. E* **1997**, *56*, 6620−6632. Öttinger, H. C.; Grmela, M. *Phys. Rev. E* **1997**, *56*, 6633−6655.
(55) Öttinger, H. C. *Beyond Equilibrium Thermodynamics*; Wiley-Interscience: New York, 2004.
(56) Eslami, H.; Grmela, M.; Bousmina, M. *J. Rheol.* **2007**, *51*, 1189−1222.

(57) Rajabian, M.; Naderi, G.; Carreau, P. J.; Dubois, C. *J. Polym. Sci., Part B: Polym. Phys.* **2010**, *48*, 2003−2011.
(58) Eslami, H.; Grmela, M.; Bousmina, M. *Rheol. Acta* **2009**, *48*, 317−331.
(59) Beris, A. N.; Edwards, B. J. *Thermodynamics of Flowing Systems with Internal Microstructure*; Oxford University Press: New York, 1994.
(60) Stephanou, P. S.; Baig, C.; Mavrantzas, V. G. *J. Rheol.* **2009**, *53*, 309−337.
(61) Stephanou, P. S. *Development of scale-bridging methodologies and algorithms founded on the outcome of detailed atomistic simulations for the reliable prediction of the viscoelastic properties of polymer melts*; Ph.D. Thesis, University of Patras (Greece), 2011.
(62) Ilg, P.; Kröger, M. *J. Rheol.* **2011**, *55*, 69−93.
(63) Beris, A. N. *J. Non-Newtonian Fluid Mech.* **2001**, *96*, 119−136.
(64) Kröger, M.; Hütter, M. *Comput. Phys. Commun.* **2010**, *181*, 2149−2157.
(65) Öttinger, H. C. *MRS Bull.* **2007**, *32*, 936−940.
(66) Edwards, B. J.; Beris, A. N.; Öttinger, H. C. *J. Non-Equilib. Thermodyn.* **1998**, *23*, 334−350.
(67) Edwards, B. J. *J. Non-Equilib. Thermodyn.* **1998**, *23*, 301−333.
(68) Huh, J.; Ginzburg, V. V.; Balazs, A. C. *Macromolecules* **2000**, *33*, 8085−8096. Ginzburg, V. V. *Macromolecules* **2005**, *38*, 2362−2367.
(69) Stephanou, P. S.; Mavrantzas, V. G.; Georgiou, G. C. Unified model for the microstructure, phase behavior, and rheology of polymer nanocomposites from nonequilibrium thermodynamics. *ACS Nano* **2014**, to be submitted.
(70) Rubinstein, M.; Colby, R. H. *Polymer Physics*; Oxford University Press: London, 2003.
(71) Edwards, B. J.; Dressler, M.; Grmela, M.; Ait-Kadi, A. *Rheol. Acta* **2003**, *42*, 64−72.
(72) Folgar, F.; Tucker, C. L. *J. Reinf. Plast. Compos.* **1984**, *3*, 98−119.
(73) Letwimolnun, W.; Vergnes, B.; Ausias, G.; Carreau, P. J. *J. Non-Newtonian Fluid Mech* **2007**, *141*, 167−179.
(74) Li, Y.; Kröger, M.; Liu, W. K. *Soft Matter* **2014**, *10*, 1723−1737.
(75) Krieger, I. M.; Dougherty, T. J. *Trans. Soc. Rheol.* **1959**, *3*, 137−152.
(76) Edwards, B. J. *J. Non-Equilib. Thermodyn.* **1998**, *23*, 301−333.
(77) Khokhlov, A. R.; Semenov, A. N. *J. Stat. Phys.* **1985**, *38*, 161−182.
(78) Bird, R. B.; Curtiss, C. F.; Armstrong, R. C.; Hassager, O. *Dynamics of Polymeric Liquids*, 2nd ed.; John Wiley and Sons: New York, 1987; Vol. *1*, Fluid Mechanics.
(79) Doi, M.; Edwards, S. F. *The Theory of Polymer Dynamics*; Clarendon: Oxford, U.K., 1986.
(80) Wildemuth, C. R.; Williams, M. C. *Rheol. Acta* **1984**, *23*, 627−635.
(81) Flory, P. J. *Principles of Polymer Chemistry*; Cornell University Press: Ithaca, NY, 1953.
(82) Tanford, C. *Physical Chemistry of Macromolecules*; Wiley: New York, 1961.